NATIONAL ADVISORY COMMITTEE
FOR AERONAUTICS

TECHNICAL NOTE 3167

MAR 26 1954

THERMAL CONDUCTANCE OF CONTACTS IN AIRCRAFT JOINTS

By Martin E. Barzelay, Kin Nee Tong, and George Hollo

Syracuse University

NACA

Washington

March 1954

NATIONAL ADVISORY COMMITTEE FOR AERONAUTICS

TECHNICAL NOTE 3167

THERMAL CONDUCTANCE OF CONTACTS IN AIRCRAFT JOINTS

By Martin E. Barzelay, Kin Nee Tong, and George Hollo

SUMMARY

Tests were conducted to determine the factors influencing the thermal
conductance across the interface between 75S-T6 aluminum-alloy and AISI
Type 416 stainless-steel structural joints. The type of joints investi-
gated included: bare metal-to-metal contact; contact surfaces coated with
zinc-chromate primer; contact surfaces separated by thin foils of good
conductors (aluminum foil and brass shim stock); contact surfaces sepa-
rated by thin sheets of insulation (asbestos); contact surfaces joined
by strength-giving bonds (Redux and Metlbond); and riveted joints. The
factors investigated were heat flow, temperature drop, temperature level,
and surface condition. Contact pressure was held constant in all the
work in order to permit a thorough investigation of the other parameters.

The experimental results gave evidence for the following conclusions:

1. The thermal conductance of the interface joint increases with
the mean temperature level, while it remains approximately constant with
changes in heat flow.

2. Thin foils of good conducting materials inserted between the
interfaces improve the heat transfer noticeably.

3. Common strength-giving bonding materials produce joints with
very poor thermal conductance.

4. It appears that across the interface joints none of the three
modes of heat transfer (namely metal-to-metal conduction, air-film con-
duction, and radiation) has any predominance over another. Furthermore,
it can be seen that there is an interdependence among these three modes
which has not previously been recognized.

INTRODUCTION

Before calculating thermal stresses in aircraft structures encountered
in the high-speed flight regime, it becomes necessary to determine temper-
ature distributions. The temperature distribution in complex structures

depends on, among other things, the thermal bond between adjacent struc-
tural parts. Determination of thermal bond involves essentially an
evaluation of the conductance of the joint, or the reciprocal quantity
known as thermal contact resistance. It is, therefore, of considerable
importance to establish values of thermal conductance for types of joints
in common use in aircraft structures and to establish laws which govern
conductance across an interface.

A survey of the literature indicates some introductory work in this
field. Jacobs and Starr in reference 1 investigated the thermal conduct-
ance of interface joints between gold, silver, and copper in a vacuum
as a function of pressure at room temperature and at the temperature of
boiling nitrogen. In reference 2, Brunot and Buckland determined the
thermal resistance of joints at the interface of laminated and cold-rolled
steel under various contact pressures and surface roughnesses. In refer-
ence 3, the thermal resistance of low-carbon steel joints was measured by
Kouwenhoven and Potter at two temperature levels for various pressures
and surface roughnesses. The temperature drop across the interface was
not a parameter in these tests. Weills and Ryder in reference 4 present
measurements of thermal resistance for dry and oil-filled joints of var-
ious materials as a function of pressure, surface finish, and temperature.
Heat flow and temperature drop were partially investigated as parameters.

It was the purpose of the present experimental study to determine the
effect of certain factors which influence thermal conductance across the
interface of structural joints, including types of joints not heretofore
investigated. The factors included were heat flow, temperature drop,
temperature level, and surface condition. Despite its importance as a
parameter in contact conductance, contact pressure was held constant in
the work reported herein in order to permit a thorough investigation of
other parameters.

This investigation, conducted at Syracuse University, was sponsored
by and conducted with the financial assistance of the National Advisory
Committee for Aeronautics. The authors wish to thank Mr. Joseph G. Cady
for his assistance in the development of test equipment and procedures
and Mr. Robert Lester for his assistance in conducting the test program.

SYMBOLS

c   constant in modified Stefan-Boltzmann law

h   conductance at interface, $Q/\Delta t$, Btu/(hr)(sq ft)($^\circ$F)

K   thermal conductivity, Btu/(hr)(ft)($^\circ$F)

n   exponent in modified Stefan-Boltzmann law

Q   heat flow, Btu/(hr)(sq ft)

r   thermal resistance of joint, $1/h$, (hr)(sq ft)($^{\circ}$F)/Btu

T, t   temperature, $^{\circ}$F abs (or $^{\circ}$R) and $^{\circ}$F, respectively

T_m, t_m mean interface temperature, $^{\circ}$F abs (or $^{\circ}$R) and $^{\circ}$F, respectively

ΔT, Δt temperature drop at interface, $^{\circ}$F abs (or $^{\circ}$R) and $^{\circ}$F,
                   respectively

x   distance in direction of heat flow, ft

ϵ constant in equation (8)

λ constant of proportionality

ν absolute or dynamic viscosity of air, slugs/ft-sec

DESCRIPTION OF APPARATUS

A general view of the test installation is shown in figure 1, and
the heating assembly and radio-frequency coil are shown in a close-up in
figure 2. In both of these figures the insulation and the containers for
the insulation have been removed. Details of the heating assembly are
presented in figure 3.

The apparatus used can be divided into the following groups:

(1) A heat source to furnish the heat input
(2) A heating head at high temperature to serve as a heat reservoir
(3) A "heat meter" to measure the heat flow
(4) A pair of specimens to provide the interfaces to be studied
(5) A cooling head at low temperature
(6) A heat sink or coolant to maintain the cooling head at low
       temperature
(7) Insulation and heat guard
(8) Temperature recording devices and controls

A description of each of the above items follows:

(1) Heat source: An electronic induction heater provided a maximum
output of 15 kilowatts by generating 225 amperes of radio-frequency cur-
rent at 510 to 540 kilocycles. The desired output was regulated by on-
and-off cyclic switching.

(2) Heating head: The heating-head assembly shown in figures 4(a) and 4(b) consists of a heavy stepped cylinder of impure copper with a stainless-steel plug. This combination furnished the proper resistive and inductive impedance to load the heater. The smaller portion of the copper cylinder which protruded below the heater coil served to minimize the skin effect in induction heating. The whole assembly provided enough thermal inertia to steady the heat flow to the specimens as the radio-frequency heater was switched on and off. The temperature at the lower end of the heating head was continually recorded by means of a Chromel-Alumel thermocouple connected to a recording potentiometer.

(3) Heat meter: The heat meter, or rather the heat-flow meter, consisted of a cylindrical piece of electrolytically pure copper 3 inches in diameter and 4 inches long inserted between the heating head and the upper specimen. A number of thermocouples were installed near the top and the bottom surfaces of the cylinder. These were connected to form a thermopile which gave the average temperature gradient in the cylinder. Thermocouples at the center of the cylinder measured the average temperature of the cylinder. The heat flow is computed from the conductivity of pure copper corresponding to the average temperature and the observed temperature gradient.

(4) Specimens: The specimens are described in detail under "Description of Specimens."

(5) Cooling head: The cooling head consisted of a copper cylinder with a central axial hole and a number of small radial holes as shown in figure 4(c). The radial holes were threaded and could be plugged by machine screws. The coolant was admitted at the bottom of the cylinder and flowed upward and outward through tiers of unplugged holes. The location and the number of holes left open were used as a means of regulating the cooling-head temperature.

(6) Coolants: The coolants used were compressed air and water. Compressed air was taken from a 90-psi air line of large capacity and regulated by a throttling valve. Water was pumped into the cooling head by a variable-speed positive-displacement pump, pumping from a constant head.

(7) Insulation: Except for a portion of the cooling head, the entire assembly was insulated with diatomaceous earth as seen in figure 3. This insulating material was held in place by a container made of galvanized iron and asbestos boards. The galvanized iron formed the lower part of the container which was away from the heating coil. Despite the distance from the coil, the galvanized iron was heated up somewhat by induction and thus it indirectly served as a guard to minimize the radial heat flow from the specimens and heat meter inside, through the insulation.

(8) Temperature measuring devices: All temperatures, except that of the heating head, were measured by iron-constantan thermocouples connected to a self-compensating potentiometer.

TEST PROCEDURE

Theoretical Basis

From the basic Fourier equation, the steady-state heat flow at any part of the heat path is given by

$$Q = K \frac{dt}{dx} \tag{1}$$

If the thermal conductance of the interface is defined as

$$h = \frac{Q}{\Delta t} \tag{2}$$

then

$$h(\Delta t) = K \frac{dt}{dx} \tag{3}$$

or

$$h = K \frac{dt}{dx} \Big/ \Delta t \tag{4}$$

The thermal resistance is defined as

$$r = \frac{1}{h} \tag{5}$$

The temperature at the boundary of a specimen can be obtained by extrapolating the temperature-distance relation existing in the interior of the specimen. The temperature drop across the interface Δt is thus determined. In equation (4) the product $K \frac{dt}{dx}$ is the heat flow per unit area. This can be obtained by measuring the temperature gradient in the pure copper and multiplying this gradient by the mean conductivity of pure copper.

Description of Specimens

The test specimens which were used to provide the interfaces for testing were paired 75S-T6 aluminum-alloy or AISI Type 416 stainless-steel blocks 3 inches in diameter and approximately 1 inch thick. The types of joints represented by the specimens included: bare metal-to-metal contact; contact surfaces coated with zinc-chromate primer; contact surfaces separated by thin foils of good conductors (aluminum foil and brass shim stock); contact surfaces separated by thin sheets of insulation (asbestos); contact surfaces joined by strength-giving bonds (Redux and Metlbond); and riveted joints. The surfaces used in testing were classified, where pertinent, as to surface roughness as established by the Brush surface analyzer and as to flatness by comparison with a standard surface plate. The specimens with surfaces termed "as received" were cut out from hot-rolled flat bar stock; the test surfaces were cleaned but not ground or polished in any way. The surfaces of all other specimens were ground to the desired surface roughness on a Blanchard surface grinder. In joints with bare metal-to-metal contact the average surface roughness ranged from 6 to 120 microinches root mean square. The average flatness of the interfaces was ±0.0002 inch except for those tested in the as-received condition. Pertinent information about interface characteristics, sandwich materials, and riveted specimens is given in table I.

Thermocouple Technique

Temperatures were determined in the specimens and in the heat meter by means of iron-constantan thermocouples. Wires of Brown and Sharpe gage 30, the smallest wire practicable, were chosen to minimize the instrumentation error. After the thermocouple bead was formed by a special direct-current welder, the length of the thermocouple which was to lie within the specimen was dipped in Glyptal lacquer to provide protection and insulation. Each thermocouple was then inserted in an 0.046-inch-diameter hole drilled to the proper depth and filled with wet copper dental cement which when hardened served to hold the thermocouple in place and provide good heat conduction. The various possible thermocouple locations in a pair of specimens (or in rivets where appropriate) are shown in figure 5.

In determining temperature gradients the temperature at a given transverse section through a specimen or heat meter was found from either a differentially connected thermopile as shown in figure 6(a) or from the average of individual thermocouples connected as in figure 6(b).

Temperatures of the upper and lower specimen interfaces were obtained by extrapolation of readings of thermocouples (or thermopiles) installed close to the interface. The extrapolation was made possible by installing

an additional set of thermocouples in the specimens some distance away from the interface to obtain the temperature gradient existing in the specimens.

Conduct of Tests

The equipment was assembled as described above. All interface junctions were thoroughly cleaned with alcohol and acetone. Thin aluminum foil was placed between all contact surfaces, except the interfaces to be tested, to reduce undesirable temperature drops. Heat was then applied and the specimens were brought up to the maximum temperature to be tested. This procedure was intended to dry the insulation and drive off any volatile material remaining on the interfaces after cleaning or in the thermocouple cement. The assembly was then allowed to cool to room temperature.

Despite its importance as a parameter in contact conductance, contact pressure was held constant at approximately 7 psi in all the tests in order to permit a thorough investigation of the other parameters.

After the preliminary heating, the actual test began with a low heat flow and at a low mean interface temperature level. With air as coolant flowing at a low rate through the lower tier of holes in the cooling head, the specimens were brought up to the desired temperature level gradually. When the desired temperature was reached the heat input was reduced to a steady-state heat flow. This was achieved by adjusting the relative durations of heater-on and heater-off periods in a 120-second cycle. The heating-head temperature which was continuously recorded gave a rough indication of the direction of the necessary adjustment in the heating cycle for reaching and maintaining a steady-state heat flow. There was, of course, a time lag between the temperature variation in the heating head and in the specimen which had to be taken into account. When a steady state was finally obtained, as evidenced by constant temperatures for a reasonable period of time, two successive sets of thermocouple readings were taken to make sure the steady state was maintained.

In achieving a steady state a small adjustment was occasionally found to be necessary to bring the temperature drop across the interface within the desired range. This could be done by adjusting the rate of coolant flow as well as its passage through the cooling head.

Tests with other interface temperatures and other temperature drops across the interface were performed in the same manner. The coolant (air or water), the flow rate of the coolant, and the coolant exit passage location controlled the cooling-head temperature, while the off and on proportion of the heating cycle controlled the heating-head temperature. These in turn determined the temperature level and the temperature drop at the interface.

For a given set of specimens the test results could be reproduced fairly well after the specimens had been brought up to high temperature once. This was true only when the assembly was not disturbed. Rotating the surfaces with respect to each other even slightly produced appreciable scatter in the results.

PRECISION OF DATA

It is virtually impossible to state in fixed percentages the errors in the recorded readings, since there could be many sources of error with varying degrees of influence for different sets of readings. It is, therefore, appropriate to discuss individually these sources of error and their influence on the final results.

The most important source of error was in the thermocouple readings from which, directly or indirectly, all the numerical results were obtained. When these readings were used to compute either the temperature drop or the temperature gradient, the absolute errors in individual temperature readings were of little consequence so long as they were uniform in all thermocouples. When the readings were used to determine the temperature levels in the heat path, the physical phenomena involved were not sufficiently sensitive for any normal error in the instruments to be of consequence. The thermocouples for any set of specimens were made of wire from the same lot and read on the same potentiometer. On account of this uniformity in the wire, the sensitivity of the potentiometer became the determining factor in the accuracy of the computed temperature gradients. With the length of thermocouple wire used, the sensitivity of the potentiometer is ± 0.02 millivolt, or $\pm 2/3^{\circ}$ F. By taking the average of several readings, the maximum error originating in the potentiometer, and reflected in the temperature drop measured, should be about $\pm 1^{\circ}$ F. The significance of this error depended on the magnitude of the temperature drop.

The second source of error was in the nonparallel heat flow which could be caused by (a) heat loss in the radial direction and by (b) nonuniformities in the heat path. The quality and the thickness of insulation used were such that radial heat loss to the surroundings was insignificant. Although no measurement was made to determine this loss, there was evidence for the above assertion in that the metal container holding the insulation was only slightly warm to the prolonged touch except when it was being periodically heated by stray induction field from the heating coil. The nonuniformity of heat flow is of two origins. The first is the nonuniformity inherent in the very nature of contact resistance. The second is the disturbance created by the thermocouple insertion. Nothing can be done with the first. The second can be and was minimized as previously described in the section "Thermocouple Technique."

The maximum variation in the readings of thermocouples installed at the same level was about 8° F in aluminum specimens and 15° F in stainless-steel specimens, and about 3° F in the copper heat meter. Most of the experiments were carried out with these thermocouples in a differential thermopile and, therefore, the variation in readings of the individual thermocouples at the same level was not known. The value that prevailed was probably much less than the maximum figures quoted above. It seems certain, however, that most of the observed variation was due to the previously discussed nonuniformity of heat flow except perhaps at levels near the cooling head, where the top 2 inches were insulated in the same manner as the heat meter and specimens, but the lower part was exposed and may cause some irregularities in heat flow at levels just above. However, the temperatures and thus the temperature gradient along the heat path were determined from the average readings of several thermocouples installed at different points at a given level, and this averaging process served to alleviate the significance of the unavoidable nonuniformity.

Precise measurement of the axial location of thermocouple beads was necessary to the calculation of temperature gradient. The thermocouple beads were assumed to be located at the same level as the mouth of the holes. This assumption involved a slight error as the drilled holes could not be exactly straight. A few specimens were cut apart after the tests to determine the exact bead locations. It was found that there was never more than 0.01 inch difference between the level of the bottom and the mouth of a hole. This difference was considered to be of little consequence.

Other sources of error were believed to be insignificant in comparison with those discussed above. These sources included (a) variation in coolant temperature during the period when the temperatures were being recorded, (b) heating of the specimens due to stray induction field, and (c) heat loss along the thermocouple wire.

RESULTS

The results of the tests made to determine the conductance of various interface configurations are given in table II. This table records the temperature drop across the interface, the quantity of heat flowing, and the interface conductance for each test configuration (with a given test number) at a series of mean interface temperatures.

The mean temperature level of the interface ranged from 150° to 500° F in different sets of specimens. Heat flow of approximately 2,000 to 50,000 Btu/(hr)(sq ft) produced temperature drops across the interface ranging from a few degrees to about 150° F for bare joints and those with good conducting foils and to about 350° F for insulating types of joints.

The results reported can be used quantitatively in actual engineering analysis provided that most of the idealized experimental conditions are closely duplicated in an actual design. Otherwise, they serve to indicate qualitatively the relationship between the amount of heat transfer and the various pertinent factors in an actual structural joint.

Typical sets of data from table II were plotted in figure 7 for three different types of joints in order to show the relationship of thermal conductance to temperature drop for various mean interface temperatures. It may be seen in figure 7 that there is a slight decrease in interface conductance h with increasing temperature drop Δt across the joint. This tendency prevailed everywhere when h was plotted against Δt for other sets of specimens. It was assumed that a part of this decrease was due to heat losses and an attempt was made to verify this assumption by repeating several tests with the heat meter beneath the specimens instead of above the specimens as in figure 3. No satisfactory conclusion was reached because of the difficulty in maintaining an identical contact of surfaces while moving the heat meter. Further experimentation is needed to clarify this point since up to now no valid physical explanation has been found for the variation in interface conductance with temperature drop across the joint. It should be noted, however, that the conductance of the interface joint remains approximately constant with changes in heat flow (table II).

It may also be seen in figure 7 that the conductance at a joint increased with mean interface temperature. This increase, apparent in figure 7 for the three typical joints for which the data were plotted, is clearly seen from figure 8, which will be discussed in the following paragraphs.

The joints tested in this program were classified by types and the complete data for related types of joints were plotted in groups of curves in the different graphs of figure 8. These graphs represent the primary body of data in this program as taken from table II.

The most noticeable feature of all the curves of figure 8 is the increase of conductance with the increase in the mean interface temperature. This tendency is reconcilable with theoretical considerations as is discussed in the following section.

The root-mean-square surface-roughness reading was considered as a parameter for the aluminum-aluminum joints in figure 8(a). Other things being equal, it is expected that the smoother the interfaces in contact the higher will be the conductance. In this connection, it may be remarked that although root-mean-square reading in itself is not an exact criterion of roughness it may be considered so when all surfaces are machined in the same way and hence have similar "wave forms." This tendency in the variation of conductance with surface roughness is generally borne out in the results obtained. There were a few instances of discrepancies,

however, which arose from the fact that an important factor, the flatness of the surfaces, was also involved but unaccounted for. For instance it is seen that as-received surfaces which had the lowest root-mean-square readings had much poorer conductance than the machined surfaces with higher root-mean-square readings, by a margin larger than what may be ascribed to the thin oxide scale on the as-received surfaces.

Unfortunately the flatness of a surface cannot be meaningfully represented by a numerical parameter. Although the maximum deviation in the surface from an ideal plane is some measurement of flatness, it gives no information concerning the condition of mating. Thus the same pair of surfaces mated in different ways yielded different results (tests 1 and 4); and sometimes surfaces with lower root-mean-square readings produced lower conductance values than another pair of surfaces with slightly higher root-mean-square readings (tests 5 and 6).

It is seen then that there are three important factors affecting the character of the contact and thus the conductance of the joint. These factors are (1) the roughness as measured by root-mean-square readings, (2) the flatness as measured by the maximum deviation in the surface from an ideal plane, and (3) the way in which the surfaces are mated. Where the effects of items (2) and (3) are essentially alike the data of figure 8(a) indicate that the smoother the interfaces in contact, the higher will be the conductance.

The conductance data for aluminum-aluminum joints with various sandwich materials between the joints are presented in figure 8(b). The good conductors such as aluminum foil are seen to give conductances almost 10 times those for the poor conductors such as asbestos, Redux cement, and Metlbond. What is of greater interest, however, is that the aluminum-foil sandwich shows as good conductance values as the best plain aluminum surfaces (as seen in fig. 8(a)) despite the interposition of an additional layer of material and an additional interface. A part of the improved conductivity may be ascribed to the better contact provided by the thin foil compared with that of solid blocks.

Data for the riveted aluminum specimens are given in figure 8(c). For these specimens, the conductance calculated was based on the total cross-sectional area of the specimens, that is without subtracting the rivet area, which accounted for less than 1 percent of total area per rivet. Owing to the discontinuity created by the rivet, the heat flow became nonparallel near the rivet. Therefore, the conductance value determined can be considered only a nominal value.

The difference in conductance between the one- and three-rivet specimens does not seem to be significant, despite the additional heat paths provided by two more rivets. As noted in the discussion above the flatness and mating of the surfaces were probably of significance despite

the similarity in root-mean-square roughness for the one- and three-rivet specimens. A definitive statement cannot be made at this time since insufficient data are available.

The behavior of the riveted specimens indicated by curves A and B of figure 8(c) is also of considerable interest. As this set of speci- mens was heated to a mean interface temperature above 400° F an appre- ciable drop in conductance was noted. Upon reheating, as seen in curve B, the specimens behaved in an entirely different manner, indicating that new conditions had been established in the joint. Several explanations may be advanced for this behavior. The most logical of these assumes that, as the setup was heated and the top specimen expanded more than the bottom one, the rivet was able to slip in the top specimen while still clamped in the bottom. Since at the same time the portion of the rivet at the interface could expand the condition was finally reached where slight separation of the interface could take place. At this time the conductance would fall off sharply as observed (curve A). Upon cooling the interface, the gap would be closed, but the mating conditions would not be exactly the same as before. The set of specimens would then behave as a new set (curve B). If curve B is extrapolated it is seen to coincide with curve A at a mean temperature of 500° F, the highest point taken in the first heating. This explanation is borne out by a study of temperature distributions within the rivet and specimen, typical samples of which are shown in figures 9(a) and 9(b). In these typical samples the temperatures were those recorded before the slippage took place.

Stainless-steel and stainless-steel-sandwich conductance data are plotted in figures 8(d) and 8(e). No additional explanation of these data is necessary since the observable trends are the same as those pre- viously discussed in this section for aluminum joints.

DISCUSSION

The heat transfer across the surfaces in contact may be considered as consisting of three separate modes: (1) the heat transfer across points in actual contact, (2) the heat transfer through the thin air film by conduction (or by diffusion, to be exact), and (3) the heat transfer by direct radiation. Various investigators in the past have held dif- fering opinions about the relative importance of these three modes of heat transfer. The results of the present experimentation do not seem to indicate the predominance of any single mode.

Weills and Ryder stated in reference 4 that, since the conductivity of metallic substances is of the order of a thousand times that of air, most of the heat transfer must take place through the points of contact. However, according to Holm in reference 5, for two rigid surfaces the

actual points of contact are few and small. For heat flux to go through these few points it would have to follow devious paths and the resistance along these paths could be higher than the air gap resistance. Thus, other investigators such as Keller (ref. 6), in discussing heat transmission in strip coil annealing, state that approximately 98 percent of heat flow is by conduction across the gas film. The results of this experimentation do not seem to support this estimate.

The evidence against the predominance of any particular heat-transfer mechanism may be presented as follows. If the heat transfer takes place mainly at the actual points of contact then the so-called contact resistance is physically fictitious, for the contacts as such are imaginary fragmentary surfaces of no thickness and hence no resistance. The apparent resistance measured is due to a decrease of average temperature gradient at points away from the contact surface caused by the resistance of heat path near the surface. For a given assembly of specimens the geometrical pattern of flux lines and equipotential lines should not change with respect to either temperature level or flux density except for a small variation of conductivity of the metal at different temperatures. However, the thermal conductance of the interface, as measured, showed appreciable increase with the increase of temperature level, as previously mentioned in connection with figure 8.

Now this increase of thermal conductance seems to be qualitatively compatible with the contention that the transfer of heat takes place mainly through the air film, since according to kinetic theory of gases the thermal conductivity of air is proportional to its dynamic viscosity. For the temperature range encountered the dynamic viscosity of air can be represented by $\nu = (3.5 + 0.005t) \times 10^{-7}$ slug/ft-sec. From this it can be deduced that

$$\frac{1}{h}\frac{dh}{dt_m} = \frac{5}{3,500 + 5t_m} \; {}^{\circ}F^{-1} \tag{6}$$

by assuming the mean temperature level to be the mean temperature of the air film (see appendix A). The quantity on the left-hand side can be obtained from the experimental data and checked against the value predicted by the equation. It was found that, in the case of specimens with flat ground surfaces, the formula gave slightly lower values while for those with less flat as-received surfaces it gave values two-thirds that of the experimental results. This disparity cannot be reconciled with the belief that the heat transfer took place primarily by conduction through the air film, for in that case the formula should predict the results more closely in the case of tests with as-received surfaces where the contact was poor and, hence, the air-film conduction was more important. It should be realized that, while such indirect evidence is not sufficient to establish constructively any physical law, it does serve to discredit the validity of certain hypotheses; in this case the hypothesis is that air-film conduction is predominant.

The role played by direct radiation is also controversial because of seemingly conflicting evidence (refs. 2, 3, 4, and 6). If one assumes that the radiation is the only mechanism of heat transfer, then the conclusion is that the heat transfer should follow roughly the generalized Stefan-Boltzmann law,

$$Q = c\left(T_1{}^n - T_2{}^n\right) \tag{7}$$

with n lying between 4.6 and 5.0 (ref. 7). It was found, indeed, that the different sets of results in this experiment could be represented rather closely in this form (figs. 10(a) to 10(d)), but the value n is too small to indicate a predominance of heat transfer by direct radiation. The value of n obtained by empirical curve fitting can, however, very well be some measure of the importance of the direct radiation. A detailed discussion of this empirical relation is postponed to the end of this section.

Up to this point the discussion has been confined to examination of the possibility of any single mode of heat transfer across the interface being predominant, and it was pointed out that several of the previously mentioned investigators had attempted to estimate the relative resistance in each of the possible modes. These estimates were based upon the assumption, stated or implicit, that the heat transfer by one mode was independent of the existence and intensity of the other modes. This reasoning is perhaps summed up by the suggestion in the discussion following reference 2 that the contact resistance should consist essentially of three parallel resistances: (1) the contact resistance of the direct metallic bond, (2) the air-film resistance, and (3) the radiation resistance across the air film. But here again, as in previous estimates, application of the stated principle did not lead to agreement with data presented and explanations fell back on speculation as to whether assumptions of the relative amounts of heat transferred by each mode were correct.

In examining the previously mentioned simple analog it becomes apparent that the mutual independence of the air-film resistance and the radiation resistance might be assumed but certainly not the independence of the contact resistance and other two resistances. A more appropriate model is therefore shown in figure 11. In this model, the contact resistance does not exist explicitly. It is embodied only in the topology of the network. This dependence upon the topology together with the nonlinear character of the air-film and radiation resistances makes the separate determination of the resistances unprofitable.

The phenomenon described above can also be deduced from purely mathematical reasoning. The temperature distribution is governed by the

linear Laplace equation in the solid body and at points of contact and by the nonlinear boundary conditions at points where the surfaces are separated by air film. The problem as a whole is, therefore, nonlinear and its solution cannot be obtained by superposition.

One might argue that, if the points of actual contact are evenly distributed over the surface and the film thickness is statistically uniform, the topological structure of the domain is then more or less known. Such a distribution, however, is unlikely on rigid surfaces machined by ordinary means.

As mentioned previously, by borrowing the equation of radiation and allowing n to assume lower values, equation (7) was found to be a good empirical formula for the over-all heat transfer. The curves in figures 10(a) to 10(d) were plotted with values of n found by trial and error. The values are tabulated as follows:

Interface joint	n
Aluminum and aluminum (test 5)	3.0
Aluminum and aluminum, as received (test 7)	2.5
Stainless steel and stainless steel (test 23)	2.0
Aluminum, aluminum foil, and aluminum (test 9)	1.6

Except for the first case, it is seen that the value of n decreases with the decreasing importance of radiation relative to conduction. Various conjectures can be advanced to explain the relative order of the value n found empirically, but it was felt that there was not enough experimental evidence to elaborate at this time. It must be remarked here that the apparent "good fit" of the points to straight lines in figures 10(a) to 10(d) was to some extent due to the masking effect of the scale that had to be used in these plots.

Algebraically equation (7) is equivalent to

$$h = ncT_m^{n-1}(1 + \epsilon) \tag{8}$$

where ϵ is less than 0.001 (see appendix B for this development).

Thus the empirical relation implies that the thermal conductance h is a function of mean temperature level only, a fact only approximately true. A logarithmic plot of h versus T_m is given in figure 12. There

is an appreciable scatter in the points. Theoretically, the slope of the straight lines in figure 12 is equal to n - 1. There is, however, a difference between the values of n determined by the two different methods of plotting because, when there is a scatter of points, a curve best representing a set of points in one plot may not be mathematically equivalent to that in another plot. In conclusion, it must be emphasized that this part of the discussion was included as a possible first step in finding a usable empirical formula for the thermal conductance of surfaces in contact.

CONCLUSIONS

The following conclusions have been made upon examination of the experimental results of thermal-conductance measurements:

1. The thermal conductance of the interface joint increases with the mean temperature level, while it remains approximately constant with changes in heat flow.

2. Thin foils of good conducting materials inserted between the interfaces improve the heat transfer noticeably.

3. Common strength-giving bonding materials produce joints with very poor thermal conductivity.

4. It appears that across the interface joints none of the three modes of heat transfer (namely metal-to-metal conduction, air-film conduction, and radiation) has any predominance over another. Furthermore, it can be seen that there is an interdependence among these three modes which has not previously been recognized.

5. The results reported herein can be used quantitatively in actual engineering analysis provided that most of the idealized experimental conditions are closely duplicated in an actual design. Otherwise, they serve to indicate qualitatively the relationship between the amount of heat transfer and the various pertinent factors in an actual structural joint.

Syracuse University,
    Syracuse, N. Y., April 8, 1953.

APPENDIX A

DERIVATION OF EQUATION (6)

From the data presented graphically in reference 8, the viscosity-temperature relationship at atmospheric pressure within the temperature range encountered in this experiment can be expressed by the linear equation

$$\nu = (3.5 + 0.005t) \times 10^{-7} \text{ slug/ft-sec}$$

The mean free path of molecules in this temperature range is a few microinches. (See ref. 9.) The average film thickness is estimated to be several times the mean free path. Thus the law of conduction holds approximately, and for a given pair of surfaces the film conductance is proportional to the conductivity of the air which in turn is proportional to the viscosity. Hence,

$$h = \lambda\nu = \lambda(3.5 + 0.005t_m) \times 10^{-7}$$

where λ is the constant of proportionality. The elimination of λ leads to equation (6):

$$\frac{1}{h}\frac{dh}{dt_m} = \frac{5}{3,500 + 5t_m} \ ^\circ F^{-1}$$

APPENDIX B

DERIVATION OF EQUATION (8)

In equation (7)

$$T_1{}^n = \left(T_m + \frac{\Delta T}{2} \right)^n$$

and

$$T_2{}^n = \left(T_m - \frac{\Delta T}{2} \right)^n$$

Since $\Delta T \ll T_m$, the binomial series expansion of the above equation will converge and

$$Q = 2c \left[nT_m{}^{n-1} \frac{\Delta T}{2} + \frac{n(n-1)(n-2)}{3!} T_m{}^{n-3} \left(\frac{\Delta T}{2} \right)^3 + \ldots \right]$$

$$\frac{Q}{\Delta T} = h = cnT_m{}^{n-1} \left[1 + \frac{(n-1)(n-2)}{24} \left(\frac{\Delta T}{T_m} \right)^2 + \ldots \right]$$

or (eq. (8))

$$h = cnT_m{}^{n-1}(1 + \epsilon)$$

REFERENCES

1. Jacobs, R. B., and Starr, C.: Thermal Conductance of Metallic Contacts. Rev. Sci. Instr., vol. 10, Apr. 1939, pp. 140-141.

2. Brunot, A. W., and Buckland, Florence F.: Thermal Contact Resistance of Laminated and Machined Joints. Trans. A.S.M.E., vol. 71, no. 3, Apr. 1949, pp. 253-256; discussion, p. 257.

3. Kouwenhoven, W. B., and Potter, J. H.: Thermal Resistance of Metal Contacts. The Welding Jour., vol. 27, no. 10, Oct. 1948, pp. 515s-520s.

4. Weills, N. D., and Ryder, E. A.: Thermal Resistance Measurements of Joints Formed Between Stationary Metal Surfaces. Trans. A.S.M.E., vol. 71, no. 3, Apr. 1949, pp. 259-266; discussion, pp. 266-267.

5. Holm, R.: Electric Contacts. Hugo Gebers Förlag (Stockholm), 1946.

6. Keller, J. D.: Heat Transmission in Strip-Coil Annealing. Iron and Steel Eng., vol. 25, no. 11, Nov. 1948, pp. 60-67; discussion, pp. 67-70.

7. Jakob, Max: Heat Transfer. Vol. 1. John Wiley & Sons, Inc., 1949, p. 119.

8. Binder, R. C.: Fluid Mechanics. Second ed., Prentice-Hall, Inc., 1949, p. 63.

9. Warfield, Calvin N. (for the NACA Special Subcommittee on the Upper Atmosphere): Tentative Tables for the Properties of the Upper Atmosphere. NACA TN 1200, 1947.

TABLE I

TEST SCHEDULE AND DESCRIPTION OF SPECIMENS

Test	Specimen	Description		Flatness, μin.	Surface roughness	
		Specimen material	Sandwich material		Average root mean square, μin.	Maximum peak, μin.
1	38 and 39	75S-T6	None	....	12 and 12	....
2	34 and 35	75S-T6	None	....	30 and 30	....
3	34 and 35	75S-T6	None	....	30 and 30	....
4	38 and 39	75S-T6	None	....	12 and 12	....
5	25 and 26	75S-T6	None	±315 and 360	70 and 100	290 and 400
6	17 and 18	75S-T6	None	±320 and 160	60 and 70	220 and 360
7	46 and 47	[a]75S-T6	None	±580 and 355	8 and 8	40 and 100
8	46 and 47	[b]75S-T6	None	±580 and 355	6 and 6	60 and 70
9	38 and 39	75S-T6	Aluminum foil[c]	....	12 and 12	....
10	38 and 39	75S-T6	Aluminum foil[c]	....	12 and 12	....
11	38 and 39	75S-T6	Brass shim[d]	....	12 and 12	....
12	38 and 39	75S-T6	Zinc-chromate primer	....	12 and 12	....
13	34 and 35	75S-T6	Metlbond cement	....	30 and 30	....
14	38 and 39	75S-T6	Redux cement	....	12 and 12	....
15	38 and 39	75S-T6	Asbestos sheet[e]	....	12 and 12	....
16	44 and 45	[f]75S-T6	None	....	12 and 12	....
17	44 and 45	[fg]75S-T6	None	....	12 and 12	....
18	40 and 41	[f]75S-T6	None	....	12 and 12	....
19	36 and 37	[f]75S-T6	None	....	30 and 30	....
20	42 and 43	[h]75S-T6	None	....	12 and 12	....
21	48 and 49	Stainless steel	None	....	60 and 20	250 and 60
22	48 and 49	Stainless steel	None	....	60 and 20	250 and 60
23	52 and 53	Stainless steel	None	....	42 and 45	145 and 200
24	54 and 55	Stainless steel	None	....	40 and 30	180 and 120
25	50 and 51	Stainless steel	None	±150 and 185	120 and 100	400 and 450
26	48 and 49	Stainless steel	Aluminum foil[c]	±75 and 75	60 and 20	250 and 60
27	48 and 49	Stainless steel	Brass shim[d]	±75 and 75	60 and 20	250 and 60

[a]As received; assembled with grains parallel.

[b]As received; assembled with grains crossed.

[c]Thickness of aluminum foil, 0.0008 in.

[d]Thickness of brass shim, 0.0010 in.

[e]Thickness of asbestos sheet, 0.010 in.

[f]One rivet.

[g]Specimens reheated after test 16.

[h]Three rivets.

TABLE II

TEST RESULTS ON THERMAL-CONDUCTANCE MEASUREMENTS

t_m, °F	Δt, °F	Q, Btu/(hr)(sq ft)	h, Btu/(hr)(sq ft)(°F)	t_m, °F	Δt, °F	Q, Btu/(hr)(sq ft)	h, Btu/(hr)(sq ft)(°F)
Test 1				Test 4			
201.0	7.8	8,200	10.5×10^2	201.2	11.7	8,000	6.9×10^2
201.0	11.2	11,300	10.1	199.3	14.7	10,400	7.1
200.2	14.0	14,100	10.1	200.2	16.7	13,600	8.1
197.5	21.0	20,300	9.7	203.5	19.4	15,900	8.2
248.8	10.5	11,400	10.9	250.7	15.1	11,000	7.3
250.2	12.5	13,600	10.9	249.5	19.7	14,600	7.4
249.7	15.6	16,700	10.7	249.7	22.6	19,400	8.6
248.3	19.8	20,900	10.6	249.3	25.4	25,000	9.9
300.3	9.1	10,700	11.8	298.3	16.8	13,300	7.9
301.5	12.3	14,300	11.6	298.7	24.3	19,100	7.8
298.8	20.0	22,700	11.4	300.0	27.0	24,800	9.2
300.8	28.0	31,000	11.1	301.8	30.4	27,700	9.1
351.3	12.6	15,200	12.0	352.0	20.1	14,800	7.4
348.7	17.0	20,400	12.0	249.0	23.5	26,400	11.2
352.0	23.1	27,400	11.9	350.0	26.3	21,900	8.3
352.2	27.8	33,000	11.9	351.3	36.0	34,300	9.5
401.5	14.8	18,600	12.6	400.3	21.6	19,200	8.9
398.5	22.4	28,100	12.5	398.7	25.7	26,200	10.2
402.3	25.9	32,500	12.5	398.2	30.7	27,800	9.1
400.2	34.4	40,600	11.8	395.0	39.9	39,300	9.9
449.2	18.1	23,300	12.9	450.8	21.9	21,700	9.9
449.8	26.0	33,400	12.9	447.3	27.6	28,200	10.2
447.5	32.5	40,100	12.4	449.3	33.5	33,200	9.9
447.7	41.8	49,200	11.8	448.5	37.5	38,600	10.3
Test 2				Test 5			
199.2	10.6	10,100	9.5×10^2	199.8	6.9	5,000	7.2×10^2
202.5	14.0	12,400	8.9	199.5	13.5	8,800	6.5
198.3	18.2	16,500	9.1	200.5	20.2	12,300	6.1
203.2	21.1	19,200	9.1	202.7	25.7	15,500	6.0
251.8	6.1	6,300	10.3	249.3	10.5	7,900	7.5
250.3	11.2	11,900	10.6	246.5	17.6	11,800	6.7
252.0	17.3	17,200	9.9	246.5	24.3	15,500	6.4
250.8	24.3	23,700	9.8	253.3	29.0	18,300	6.3
299.3	8.0	9,000	11.3	297.5	14.6	11,500	7.9
303.5	12.1	13,100	10.9	295.5	21.7	16,000	7.4
303.0	20.9	22,100	10.5	298.3	28.4	19,600	6.9
302.2	27.8	29,100	10.5	298.0	35.5	23,700	6.7
352.0	9.9	11,500	11.6	350.8	12.8	11,000	8.5
350.3	19.4	22,200	11.4	353.0	18.9	15,300	8.1
347.3	25.8	29,100	11.3	350.3	25.6	20,000	7.8
350.8	30.8	34,800	11.3	349.2	33.3	23,800	7.2
398.0	13.2	16,300	12.4	397.3	18.6	15,500	8.4
402.2	17.6	22,400	12.7	396.2	24.8	20,300	8.2
401.7	22.5	28,100	12.5	398.8	37.7	29,900	7.9
402.3	27.0	33,900	12.6	401.3	48.2	35,900	7.4
450.8	11.8	15,900	13.5	448.5	17.5	17,700	10.1
451.5	18.9	24,700	13.1	451.2	29.5	27,400	9.3
452.7	26.6	34,000	12.8	450.5	41.9	36,300	8.7
449.2	35.0	45,800	13.1	450.7	52.1	45,200	8.7
Test 3				Test 6			
203.0	4.6	3,800	8.1×10^2	202.8	13.1	6,900	5.2×10^2
200.2	7.3	6,100	8.4	197.7	19.6	9,500	4.9
202.0	9.7	8,200	8.5	198.5	24.4	11,500	4.7
299.0	6.9	6,800	9.9	200.5	28.2	13,500	4.8
300.3	11.3	10,900	9.6	254.7	17.1	9,500	5.5
300.2	15.1	14,400	9.6	250.0	27.4	14,100	5.2
401.5	10.2	10,600	10.4	249.5	33.4	17,300	5.2
402.2	19.4	16,300	8.4	247.3	43.1	21,600	5.0
399.2	28.9	22,700	7.9	301.7	24.1	13,800	5.7
				302.2	29.0	16,200	5.6
				302.2	40.5	23,300	5.8

TABLE II - Continued

TEST RESULTS ON THERMAL-CONDUCTANCE MEASUREMENTS

t_m, °F	Δt, °F	Q, Btu/(hr)(sq ft)	h, Btu/(hr)(sq ft)(°F)
Test 6 - Continued			
301.7	47.4	26,900	5.7×10^2
350.2	27.6	17,500	6.4
349.2	35.9	22,100	5.99
349.5	44.1	26,600	6.04
350.0	52.4	30,900	5.90
400.0	29.6	20,300	6.83
400.0	35.9	24,300	6.76
399.7	44.7	28,900	6.46
400.7	53.2	34,600	6.51
450.5	27.5	20,700	7.53
451.3	35.1	25,900	7.38
452.3	44.3	33,100	7.47
447.7	58.8	41,600	7.07
Test 7			
202.2	18.0	6,300	3.5×10^2
199.7	26.8	8,500	3.2
200.7	32.3	10,200	3.2
201.2	40.6	12,800	3.15
248.5	25.1	8,900	3.5
247.3	34.6	11,700	3.4
248.8	41.6	13,900	3.35
250.5	47.9	16,000	3.3
300.2	27.4	10,300	3.8
301.8	48.8	17,800	3.65
299.7	59.2	21,900	3.70
298.2	86.3	30,800	3.56
350.7	35.0	14,300	4.1
350.0	52.8	21,000	4.00
350.8	63.5	25,300	4.00
350.3	75.5	30,200	4.00
401.5	37.6	16,500	4.4
400.3	52.4	22,800	4.35
397.3	63.0	27,400	4.35
403.0	80.5	35,200	4.37
452.0	39.5	18,900	4.8
449.5	51.5	24,200	4.69
451.8	61.8	27,600	4.47
Test 8			
199.7	20.7	6,000	2.9×10^2
199.2	29.6	8,300	2.8
202.2	35.6	10,000	2.8
200.2	49.1	14,000	2.8
302.2	31.3	10,300	3.3
300.3	45.6	14,700	3.22
301.2	55.1	18,000	3.27
301.8	67.4	22,100	3.29
403.2	36.3	13,800	3.8
398.5	52.6	19,800	3.77
398.5	66.2	25,500	3.86
396.7	79.5	30,900	3.88
Test 9			
201.2	5.7	5,600	9.8×10^2
200.5	9.0	8,900	9.9
199.5	11.0	10,500	9.6
199.8	15.0	14,500	9.7
252.0	7.4	8,200	11.0
249.7	12.2	12,700	10.4
250.7	14.6	15,000	10.3
248.5	20.0	20,400	10.2
301.7	10.0	11,900	11.9

t_m, °F	Δt, °F	Q, Btu/(hr)(sq ft)	h, Btu/(hr)(sq ft)(°F)
Test 9 - Continued			
299.7	15.0	16,400	11.3×10^2
300.5	17.9	19,900	11.1
300.7	23.4	25,900	11.1
350.3	11.3	13,400	11.8
348.2	15.4	18,500	12.0
352.8	18.2	22,000	12.0
352.0	25.0	28,100	11.2
401.3	10.6	13,400	12.7
396.7	15.3	18,900	12.4
398.5	20.0	24,800	12.4
399.7	26.7	32,000	12.0
Test 10			
201.7	8.5	5,800	6.8×10^2
202.0	11.1	7,900	7.1
201.0	15.8	10,700	6.8
198.3	21.7	15,400	7.1
249.5	10.0	8,100	8.1
252.7	13.5	10,700	7.9
251.0	17.5	14,000	8.0
248.8	24.2	19,000	7.8
300.8	9.8	9,700	9.9
296.8	15.0	13,900	9.3
300.7	18.0	16,900	9.4
299.2	25.6	23,500	9.2
352.2	11.8	12,500	10.6
350.0	17.0	18,600	10.9
349.8	19.8	22,000	11.1
349.2	26.3	29,000	11.0
399.7	15.0	17,900	12.0
398.0	21.2	24,000	11.3
398.0	25.6	28,400	11.1
400.0	38.1	41,400	10.9
451.2	14.8	18,400	12.5
451.3	20.9	26,500	12.7
450.3	26.1	32,500	12.5
446.8	31.0	38,400	12.4
Test 11			
200.2	7.8	5,100	6.6×10^2
200.5	15.4	8,800	5.7
201.3	19.9	11,500	5.8
198.8	29.8	17,100	5.8
250.7	11.1	7,100	6.4
247.0	17.3	10,500	6.1
250.3	21.1	13,600	6.5
250.3	36.2	22,400	6.2
302.7	13.7	9,400	6.9
299.2	20.9	13,700	6.6
302.2	26.1	17,500	6.7
298.2	39.1	26,000	6.7
348.3	16.0	11,200	7.0
349.3	26.3	18,700	7.1
348.3	36.0	25,500	7.1
350.2	49.0	35,400	7.2
400.8	18.0	14,000	7.8
399.8	23.0	18,300	8.0
400.7	36.9	31,200	8.4
399.7	51.6	41,900	8.1
450.0	20.2	18,000	9.0
451.2	29.7	26,800	9.0
451.3	48.4	42,900	8.9

TABLE II - Continued

TEST RESULTS ON THERMAL-CONDUCTANCE MEASUREMENTS

Test 12

t_m, °F	Δt, °F	Q, Btu/(hr)(sq ft)	h, Btu/(hr)(sq ft)(°F)
198.2	11.9	5,000	4.2×10^2
200.0	19.0	8,300	4.4
200.7	39.0	14,000	3.61
200.7	59.5	18,200	3.05
249.8	17.0	7,100	4.2
247.8	29.3	12,300	4.2
247.8	49.8	18,800	3.78
250.3	79.4	24,500	3.09
303.0	21.1	9,000	4.3
301.5	36.4	15,900	4.4
299.8	61.6	23,800	3.86
300.7	91.3	31,100	3.41
350.7	23.6	10,500	4.4
349.0	42.7	18,500	4.34
350.5	69.6	27,500	3.96
349.8	110.4	37,600	3.40
400.7	31.4	14,300	4.6
396.5	37.5	17,100	4.6
397.2	55.3	23,400	4.24
397.7	94.5	36,300	3.84
450.7	34.5	15,600	4.5
450.3	66.7	27,800	4.2
449.5	84.2	34,200	4.06
449.7	122.3	45,400	3.71

Test 13

t_m, °F	Δt, °F	Q, Btu/(hr)(sq ft)	h, Btu/(hr)(sq ft)(°F)
150.7	35.3	4,000	1.12×10^2
150.5	76.1	7,800	1.03
152.5	56.1	5,600	.99
200.4	59.0	5,500	.91
200.3	116.5	11,000	.94
201.5	82.7	7,500	.91
252.0	86.3	7,700	.90
247.7	154.7	14,300	.92
251.6	112.5	10,000	.89
303.2	108.0	9,000	.83
301.1	198.4	17,300	.87
302.5	143.0	12,600	.88
352.3	136.6	11,200	.82
351.9	240.6	22,400	.93
351.7	171.6	15,400	.90

Test 14

t_m, °F	Δt, °F	Q, Btu/(hr)(sq ft)	h, Btu/(hr)(sq ft)(°F)
152.3	43.2	2,200	0.50×10^2
152.3	47.9	3,200	.67
151.0	68.7	4,000	.59
151.7	88.0	5,000	.57
150.7	109.8	5,700	.52
202.8	66.0	3,800	.58
199.5	99.3	6,000	.61
203.7	121.4	7,400	.61
202.5	154.9	9,700	.62
254.5	68.5	4,400	.65
251.7	98.7	6,700	.68
252.7	124.3	8,700	.70
252.7	152.2	11,100	.73
252.3	186.7	13,500	.73
305.0	89.2	6,400	.72
303.0	122.6	8,300	.68
302.8	144.0	10,100	.70
302.0	195.1	14,000	.72
302.0	252.9	18,300	.72
349.2	114.0	7,400	.65
353.7	148.2	9,800	.66
347.5	189.1	13,300	.70
354.0	231.9	17,700	.76

Test 15

t_m, °F	Δt, °F	Q, Btu/(hr)(sq ft)	h, Btu/(hr)(sq ft)(°F)
249.5	83.8	5,100	0.61×10^2
251.0	123.3	7,500	.61
249.0	167.3	10,300	.62
252.5	195.1	12,000	.61
348.2	127.1	8,400	.66
350.0	162.7	10,700	.66
349.3	251.9	16,500	.65
350.5	287.6	18,600	.65
450.2	228.1	16,300	.71
451.5	267.6	19,000	.71
451.7	323.6	23,600	.73
447.8	343.0	24,700	.72

Test 16

t_m, °F	Δt, °F	Q, Btu/(hr)(sq ft)	h, Btu/(hr)(sq ft)(°F)
151.0	9.0	4,600	5.0×10^2
149.3	21.0	9,200	4.3
199.7	14.0	7,500	5.4
199.5	31.0	16,000	5.1
251.0	21.0	11,600	5.5
247.2	39.8	21,000	5.3
303.5	26.9	14,000	5.2
297.0	50.6	27,100	5.37
350.5	28.9	16,300	5.6
350.3	56.3	33,000	5.86
400.3	35.0	20,800	5.9
398.0	67.6	41,600	6.15
449.5	37.5	19,600	5.2
449.2	79.0	41,800	5.29

Test 17

t_m, °F	Δt, °F	Q, Btu/(hr)(sq ft)	h, Btu/(hr)(sq ft)(°F)
201.2	23.1	7,200	3.1×10^2
301.0	24.6	9,000	3.7
301.8	36.9	12,800	3.48
301.2	36.7	14,000	3.80
300.7	47.4	18,800	3.97
299.7	64.8	24,700	3.82
499.8	50.0	22,600	4.52

Test 18

t_m, °F	Δt, °F	Q, Btu/(hr)(sq ft)	h, Btu/(hr)(sq ft)(°F)
200.7	18.3	5,300	2.9×10^2
200.9	25.6	7,000	2.7
202.7	42.3	11,900	2.8
199.7	55.4	15,200	2.74
250.3	22.9	6,600	2.9
247.8	39.3	11,900	3.0
248.0	55.0	16,400	2.98
250.0	72.8	21,900	3.01
299.7	26.4	7,900	3.0
297.5	45.2	13,800	3.1
299.7	63.3	19,600	3.10
300.3	81.2	25,200	3.10
345.8	32.0	10,300	3.2
348.3	52.1	17,000	3.28
348.8	69.9	23,500	3.36
347.3	95.4	32,800	3.44
397.3	34.3	11,700	3.4
398.3	62.6	21,600	3.46
396.8	84.5	29,200	3.46
397.3	99.4	35,700	3.59
446.0	31.5	13,900	4.4
445.0	49.0	20,100	4.10
446.3	69.4	27,900	4.01
451.0	88.7	37,400	4.22

TABLE II - Continued

TEST RESULTS ON THERMAL-CONDUCTANCE MEASUREMENTS

t_m, °F	Δt, °F	Q, Btu/(hr)(sq ft)	h, Btu/(hr)(sq ft)(°F)	t_m, °F	Δt, °F	Q, Btu/(hr)(sq ft)	h, Btu/(hr)(sq ft)(°F)
Test 19				**Test 22 - Continued**			
201.5	30.5	6,700	2.2×10^2	401.2	19.8	18,200	9.2×10^2
200.8	57.2	12,300	2.14	402.3	23.8	24,800	10.4
250.7	39.7	8,700	2.2	450.2	13.2	14,800	11.2
248.3	69.5	15,900	2.29	451.0	26.2	28,300	10.8
300.6	46.8	11,100	2.38	504.1	14.4	15,000	10.4
298.6	87.0	21,600	2.49	498.3	27.4	28,300	10.3
352.2	56.6	15,100	2.66				
348.8	99.2	25,800	2.61	**Test 23**			
399.4	61.9	16,600	2.68				
397.8	114.5	32,500	2.84	200.9	6.9	3,700	5.4×10^2
451.6	69.2	20,000	2.89	199.1	10.7	6,000	5.6
447.9	130.4	39,800	3.05	200.0	14.6	8,100	5.5
				200.5	19.7	10,800	5.5
Test 20				249.3	9.5	5,300	5.6
				248.2	14.8	8,300	5.6
202.0	21.8	4,800	2.2×10^2	248.9	19.1	10,800	5.7
202.5	32.9	7,700	2.4	250.6	25.2	14,200	5.6
197.2	49.8	11,400	2.29	299.5	11.2	6,400	5.7
199.3	58.8	13,500	2.30	300.5	26.8	15,600	5.8
247.8	30.0	7,100	2.4	349.4	12.7	8,000	6.3
250.0	40.2	9,400	2.35	350.6	16.8	10,700	6.4
250.2	64.8	15,400	2.38	350.2	26.1	16,700	6.4
250.2	81.1	19,200	2.37	352.7	32.2	20,200	6.3
301.8	35.8	8,400	2.3	398.9	18.3	12,400	6.8
300.8	54.4	13,200	2.43	398.9	33.1	21,700	6.5
300.0	82.8	20,500	2.48	449.2	18.4	12,900	7.0
301.7	99.2	24,500	2.47	448.7	25.0	17,500	7.0
352.5	41.6	10,400	2.50	451.3	33.0	22,000	6.7
350.0	65.2	16,700	2.56	448.9	42.6	27,300	6.4
352.0	87.3	22,100	2.53	500.2	20.5	14,100	6.9
350.5	113.3	29,000	2.56	500.1	42.1	27,500	6.5
404.5	48.3	12,800	2.65				
398.3	66.0	17,100	2.59	**Test 24**			
403.3	102.5	27,100	2.64				
399.0	129.6	33,900	2.62	200.4	9.6	3,600	3.8×10^2
453.0	53.7	14,600	2.72	199.6	15.3	6,300	4.1
450.2	85.5	23,200	2.71	201.0	20.9	9,100	4.3
450.2	122.3	33,000	2.70	201.1	25.4	10,700	4.2
446.7	155.0	41,600	2.68	252.1	15.7	7,100	4.5
				252.2	29.7	13,300	4.5
Test 21				301.5	15.6	7,300	4.7
				301.6	24.5	10,900	4.5
201.0	2.6	3,500	13×10^2	300.2	30.0	13,400	4.5
199.3	3.3	5,100	16	299.1	38.3	16,800	4.4
351.7	4.7	6,700	14	351.2	22.1	11,100	5.0
349.8	6.5	8,800	14	350.2	37.6	19,600	5.2
350.4	6.9	9,600	14	403.4	23.6	12,600	5.3
349.5	7.9	11,800	14.8	401.0	32.9	16,800	5.1
500.7	13.0	18,500	14.3	400.3	39.8	20,000	5.0
				400.0	48.8	24,400	5.0
Test 22				453.0	29.9	16,500	5.5
				449.8	49.3	25,900	5.26
197.0	4.8	4,000	8.4×10^2	499.6	37.0	19,500	5.3
198.2	7.4	5,900	8.0	501.6	56.1	30,600	5.45
199.2	9.1	7,900	8.6				
203.5	12.4	10,000	8.1	**Test 25**			
251.7	6.7	5,800	8.6				
250.3	9.7	8,900	9.2	201.1	12.7	2,800	2.2×10^2
249.3	12.3	11,000	8.9	202.1	18.5	4,400	2.4
250.2	15.4	13,800	9.0	202.5	21.9	5,300	2.4
301.7	8.4	7,000	8.3	203.2	26.1	6,800	2.6
300.2	12.3	10,600	8.6	253.0	17.1	5,300	3.1
301.2	15.6	14,300	9.2	248.9	22.8	6,000	2.6
302.3	19.0	17,900	9.4	249.7	27.0	7,500	2.8
351.9	8.7	9,000	10.4	251.0	32.6	9,200	2.8
349.4	13.8	13,300	9.6	301.1	19.4	6,300	3.2
347.3	16.9	17,200	10.2	299.8	26.9	8,500	3.2
351.1	21.3	20,700	9.7	300.8	34.9	10,400	2.97
399.3	10.4	9,400	9.1	301.0	39.6	11,600	2.92
401.0	16.0	16,700	10.4	351.5	22.8	6,800	3.0

TABLE II - Concluded

TEST RESULTS ON THERMAL-CONDUCTANCE MEASUREMENTS

t_m, °F	Δt, °F	Q, Btu/(hr)(sq ft)	h, Btu/(hr)(sq ft)(°F)	t_m, °F	Δt, °F	Q, Btu/(hr)(sq ft)	h, Btu/(hr)(sq ft)(°F)
Test 25 - Continued				Test 26 - Continued			
349.8	31.9	10,400	3.27×10^2	452.2	9.2	12,100	13.2×10^2
352.4	37.5	12,500	3.34	450.3	13.2	16,900	12.9
348.2	44.4	14,000	3.15	449.5	16.7	21,200	12.7
404.1	27.3	9,400	3.4	448.7	20.8	26,200	12.6
398.6	50.0	17,100	3.42	501.7	10.7	15,500	14.4
454.0	31.0	11,000	3.5				
445.2	56.6	19,500	3.45	Test 27			
500.5	34.3	13,600	3.96				
497.8	62.8	23,200	3.70	201.3	6.1	3,600	5.9×10^2
				200.2	9.0	6,000	6.7
Test 26				199.7	12.2	8,900	7.3
				201.7	14.4	10,600	7.4
200.2	4.1	4,500	11×10^2	251.7	8.2	6,000	7.3
199.3	6.2	6,200	10.0	250.3	12.0	8,600	7.2
201.0	7.8	8,300	10.7	250.9	14.4	10,400	7.2
200.8	9.6	9,900	10.3	249.3	17.8	13,500	7.6
250.5	4.5	5,100	11.3	301.7	9.9	7,200	7.2
250.0	7.5	8,500	11.3	301.7	14.8	11,000	7.4
250.7	10.3	11,200	10.8	301.5	17.2	12,600	7.4
250.7	11.8	13,000	11.1	300.3	21.3	16,800	7.9
300.7	5.8	6,700	11.7	352.8	11.8	8,700	7.4
301.3	9.3	11,000	11.9	351.7	17.0	13,800	8.1
299.5	11.3	12,600	11.2	350.0	20.9	17,600	8.4
300.3	13.5	16,400	12.1	349.3	26.3	21,200	8.1
348.9	6.8	8,500	12.5	403.1	13.1	9,800	7.5
350.5	10.4	13,200	12.7	401.2	19.8	17,700	8.9
349.2	13.5	16,300	12.1	400.2	24.1	20,700	8.6
348.2	16.7	22,600	13.6	397.3	28.9	24,200	8.4
401.7	7.9	9,300	11.7	451.3	13.9	12,500	9.0
398.7	12.1	15,900	13.2	450.3	21.0	18,600	8.8
398.8	14.1	19,700	14.0	449.8	25.9	23,300	9.0
397.0	18.4	22,700	12.3	448.5	34.1	28,000	8.2
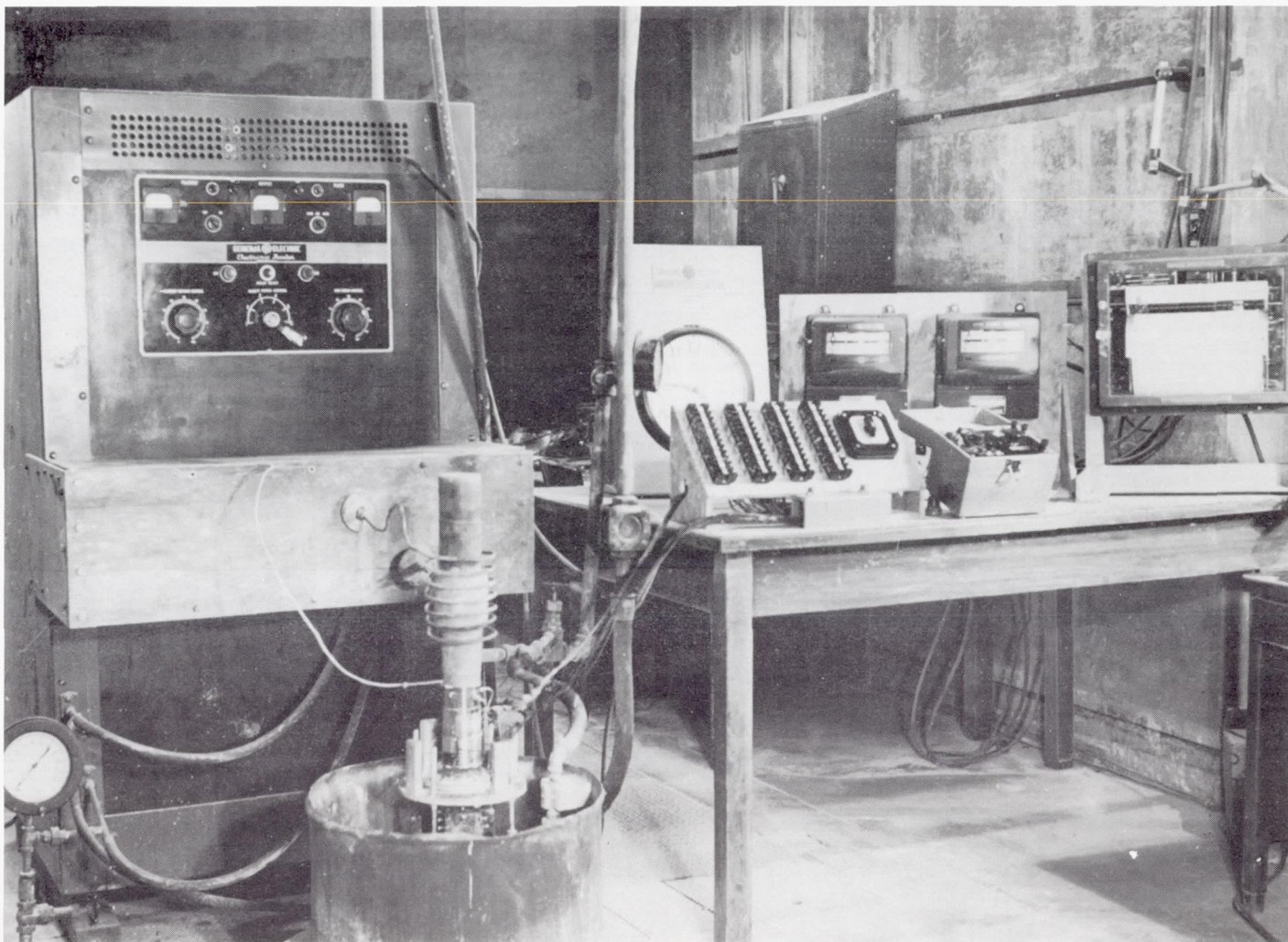
L-82077

Figure 1.- General view of test installations with insulation removed from heating assembly.
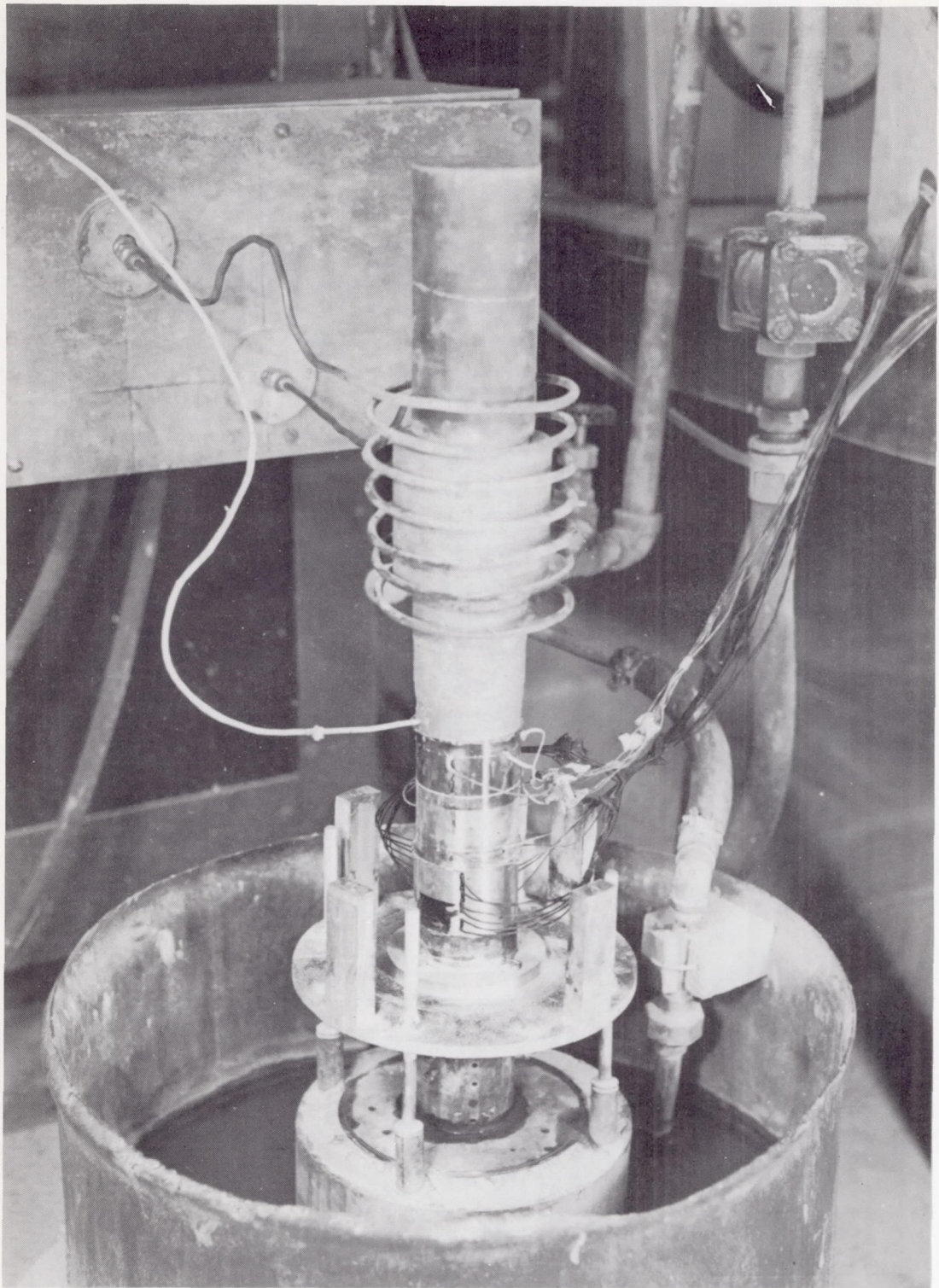
L-82078

Figure 2.- Heating assembly and radio-frequency coil.

INSULATION
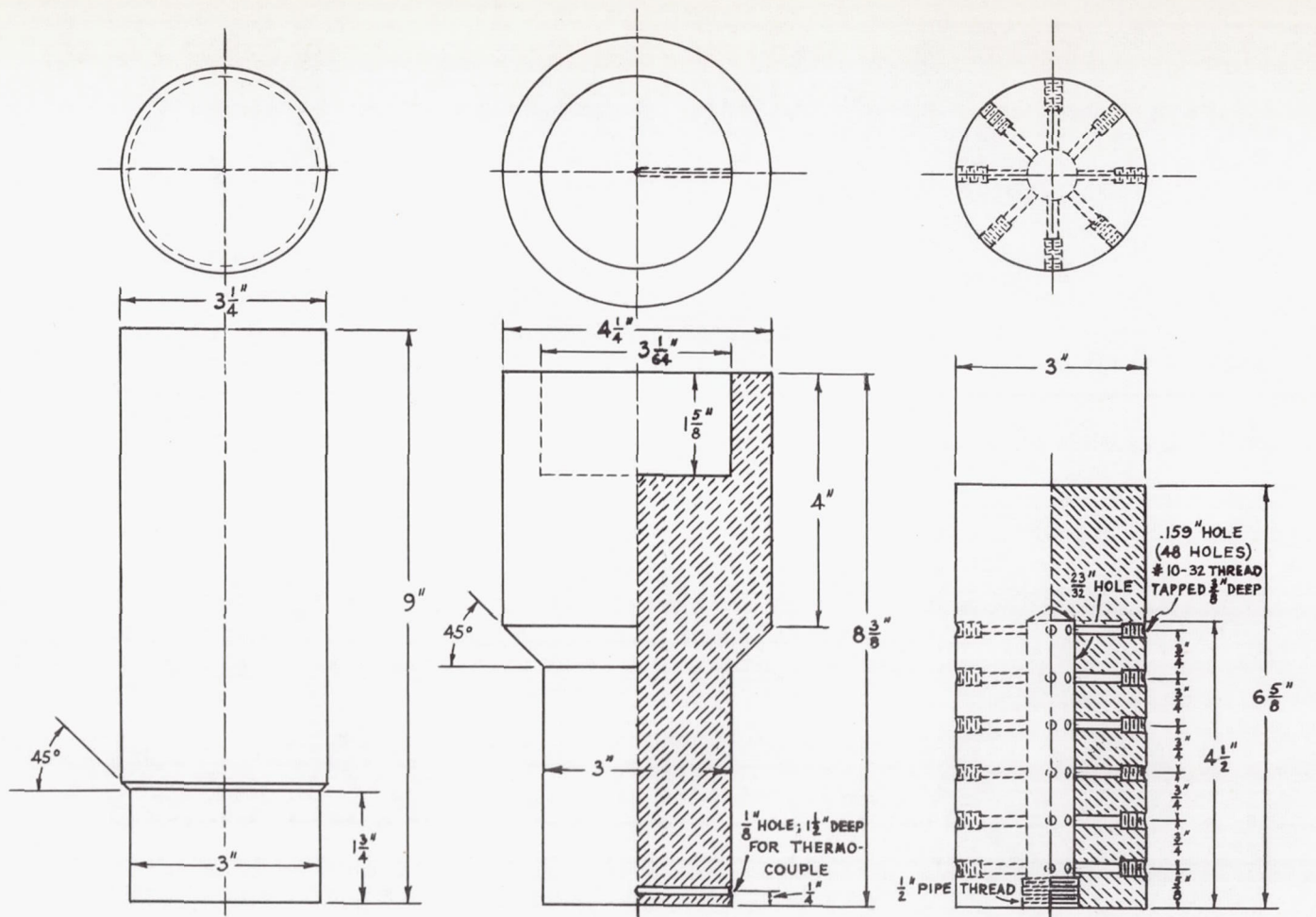
STAINLESS—STEEL CORE

SHEET ASBESTOS BOX

R.F. HEATING COIL
(WATER—COOLED)

SECONDARY HEATING HEAD
AND HEAT RESERVOIR

INSULATION

THERMOCOUPLE LEAD WIRES
TO POTENTIOMETERS

ASBESTOS
COLLAR

COOLING WATER
OR COOLING AIR

COOLING
HEAD

R.F. HEATER

INSULATION

SHEET—METAL
CYLINDER

CALIBRATED
HEAT—FLOW METER

TEST SPECIMENS

INTERFACE

DISCHARGE OPENINGS

WATER—
COLLECTING
BARREL

DRAIN

BASE

FLOOR

SCALE

0   5   10 IN.

Figure 3.- Details of heating assembly.

(a) Heating head, upper part;
material, stainless steel.

(b) Heating head, lower part;
material, chrome-plated
copper.

(c) Cooling head;
material, copper.

Figure 4.- Details of heating and cooling heads.

TYPE A : PLAIN   TYPE B : ONE RIVET   TYPE C : THREE RIVETS

TOP VIEW   TOP VIEW   TOP VIEW

SECTION G-G   SECTION H-H   SECTION J-J

INTERFACE   INTERFACE

.375"
.375"
.100"

.250"
.250"
.250"
.100"

.100"
.880"
.100"
.100"
.893"
.100"

R=.750"

DIMENSION
A   1.050" TO 1.200"
B   1.050" TO 1.200"
C   .750" TO .900"
D   .750" TO .900"
E   .040" TO .100"
F   .040" TO .100"

THERMOCOUPLE DETAIL

COPPER CEMENT
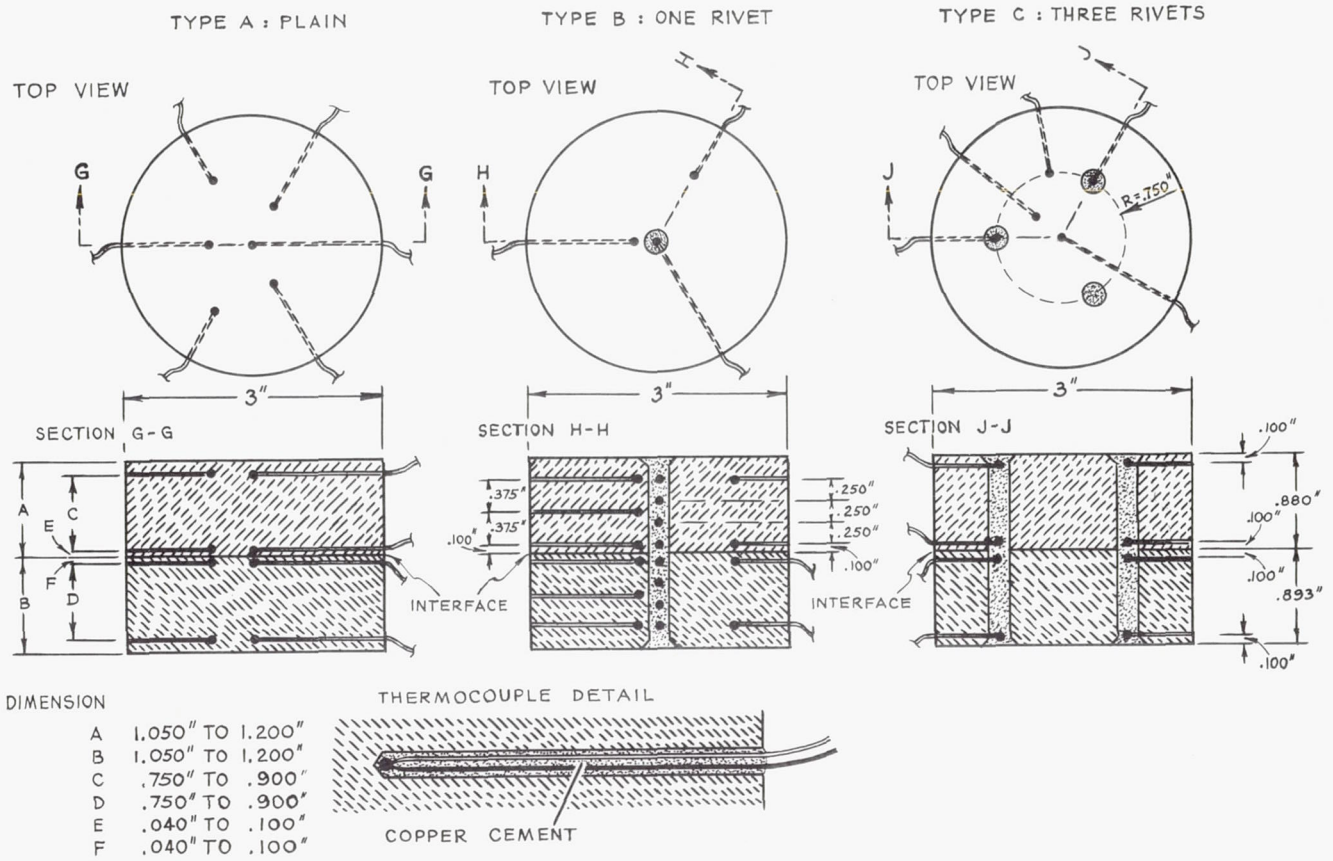
Figure 5.- Specimen and thermocouple configurations. Diameter of all
thermocouple holes is 0.046 inch (No. 56 drill). Thermocouple holes
are drilled to following depths: 5/8, 3/4, 15/16, 1, $1\frac{1}{8}$, $1\frac{1}{4}$, and
$1\frac{1}{2}$ inches.

(a) Typical differentially connected
    thermocouples.

——————— IRON

– – – – – – CONSTANTAN

INTERFACE

LEEDS &
NORTHRUP
BALANCED
THERMOCOUPLE
POTENTIOMETER

SELECTOR
SWITCH
(24 CHANNELS)
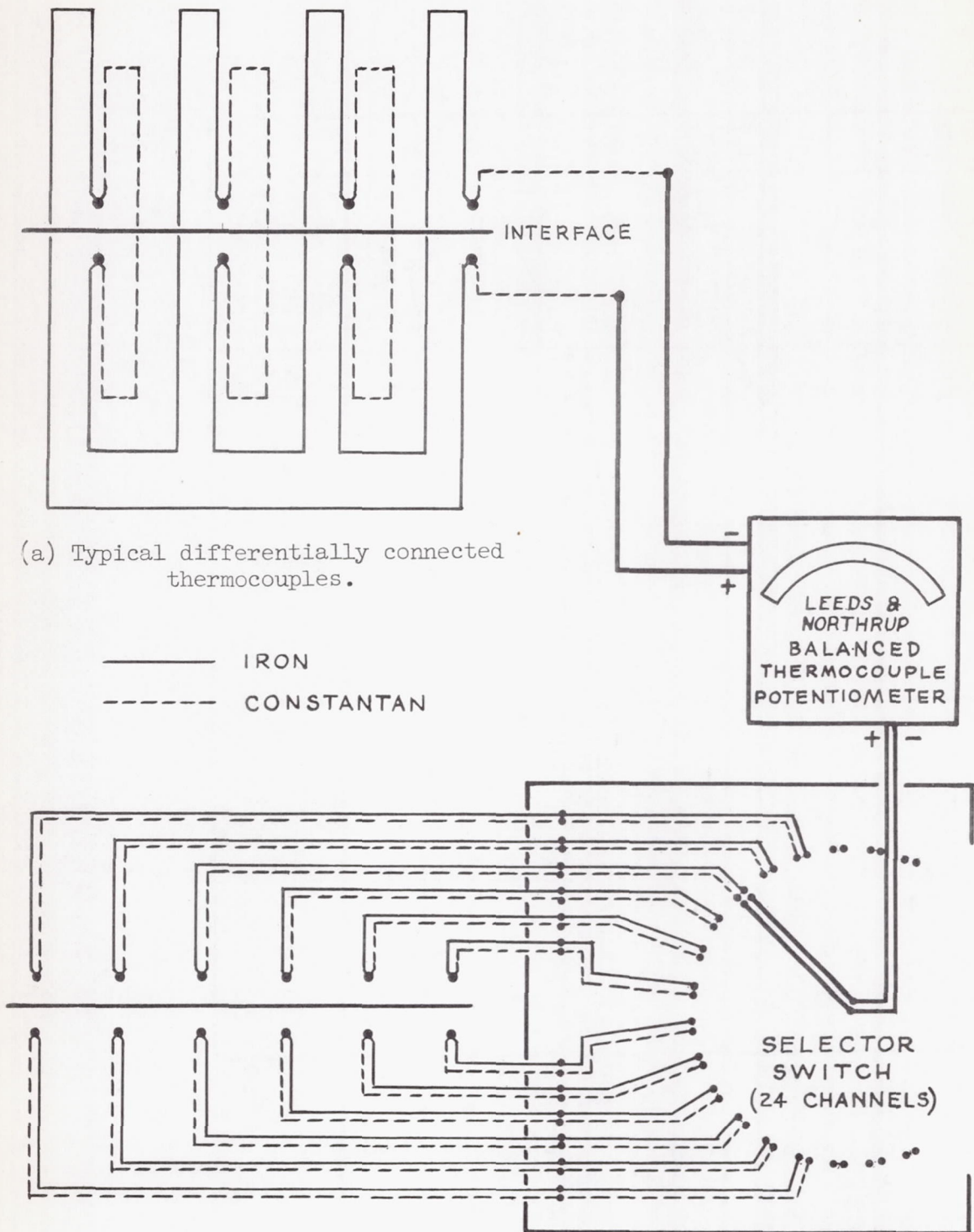
(b) Typical individual thermocouples.

Figure 6.- Thermocouple wiring diagrams.
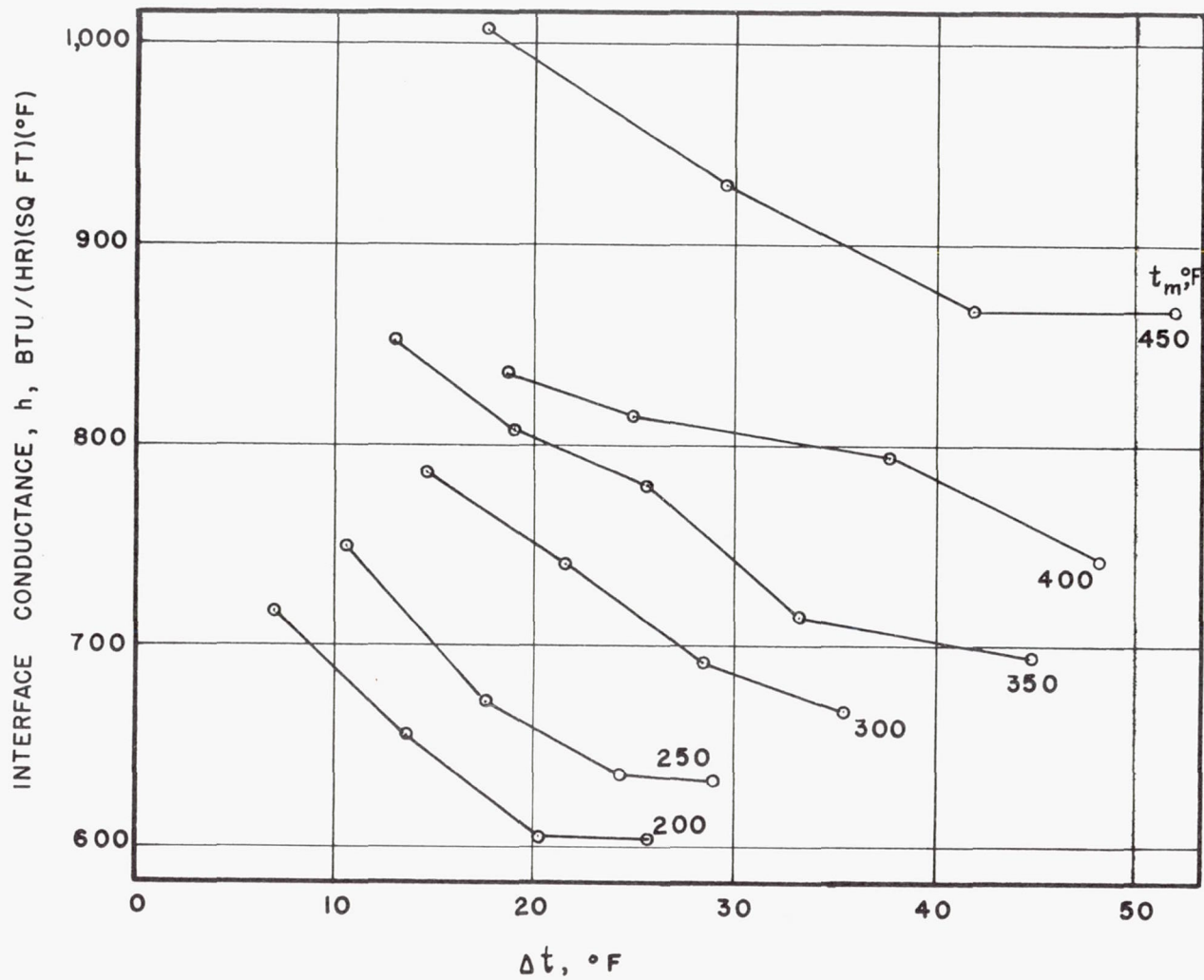
(a) Aluminum-aluminum joint (test 5).

Figure 7.- Interface conductance versus temperature drop for various mean
interface temperatures.
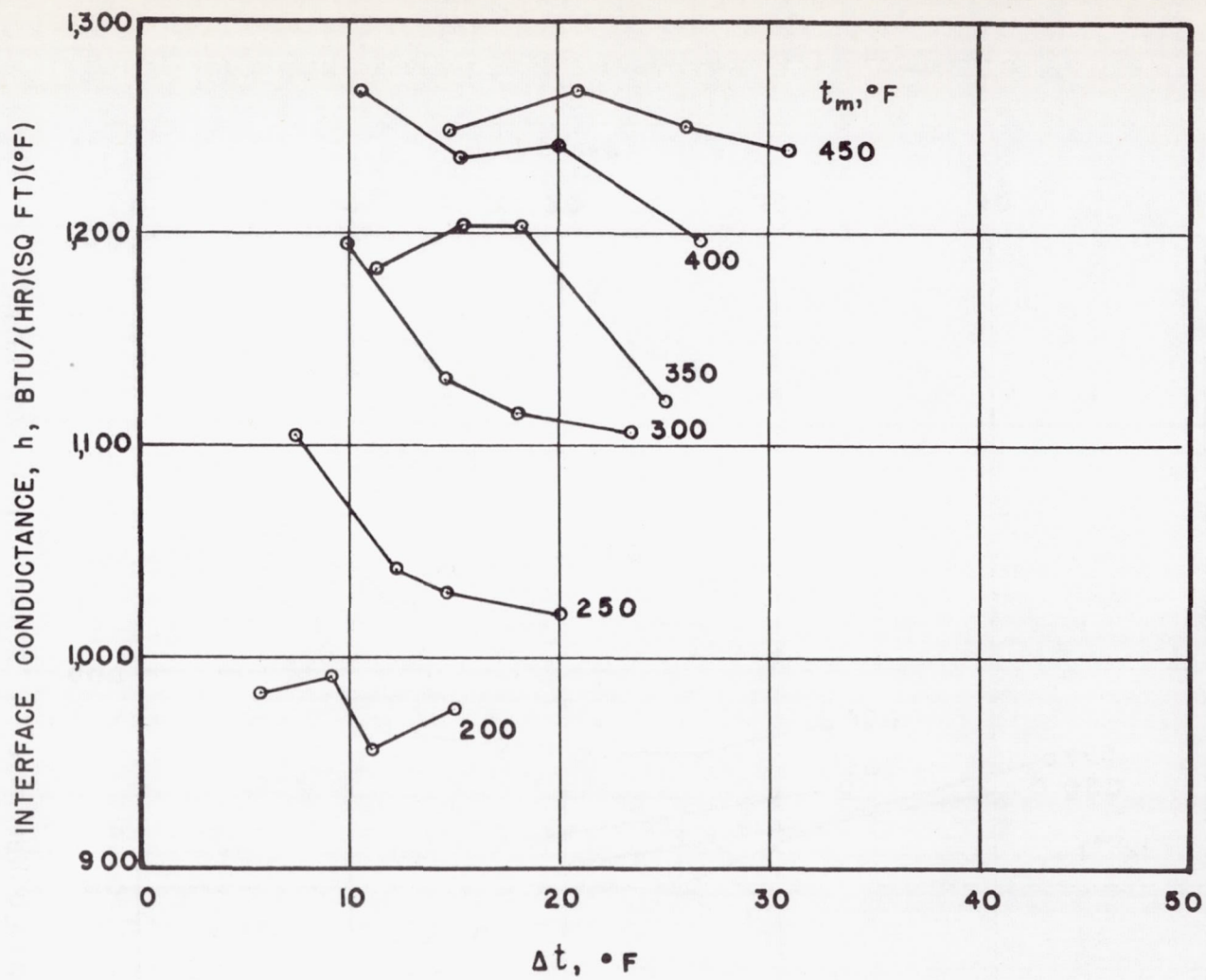
(b) Aluminum, aluminum foil, and aluminum joint (test 9).

Figure 7.- Continued.
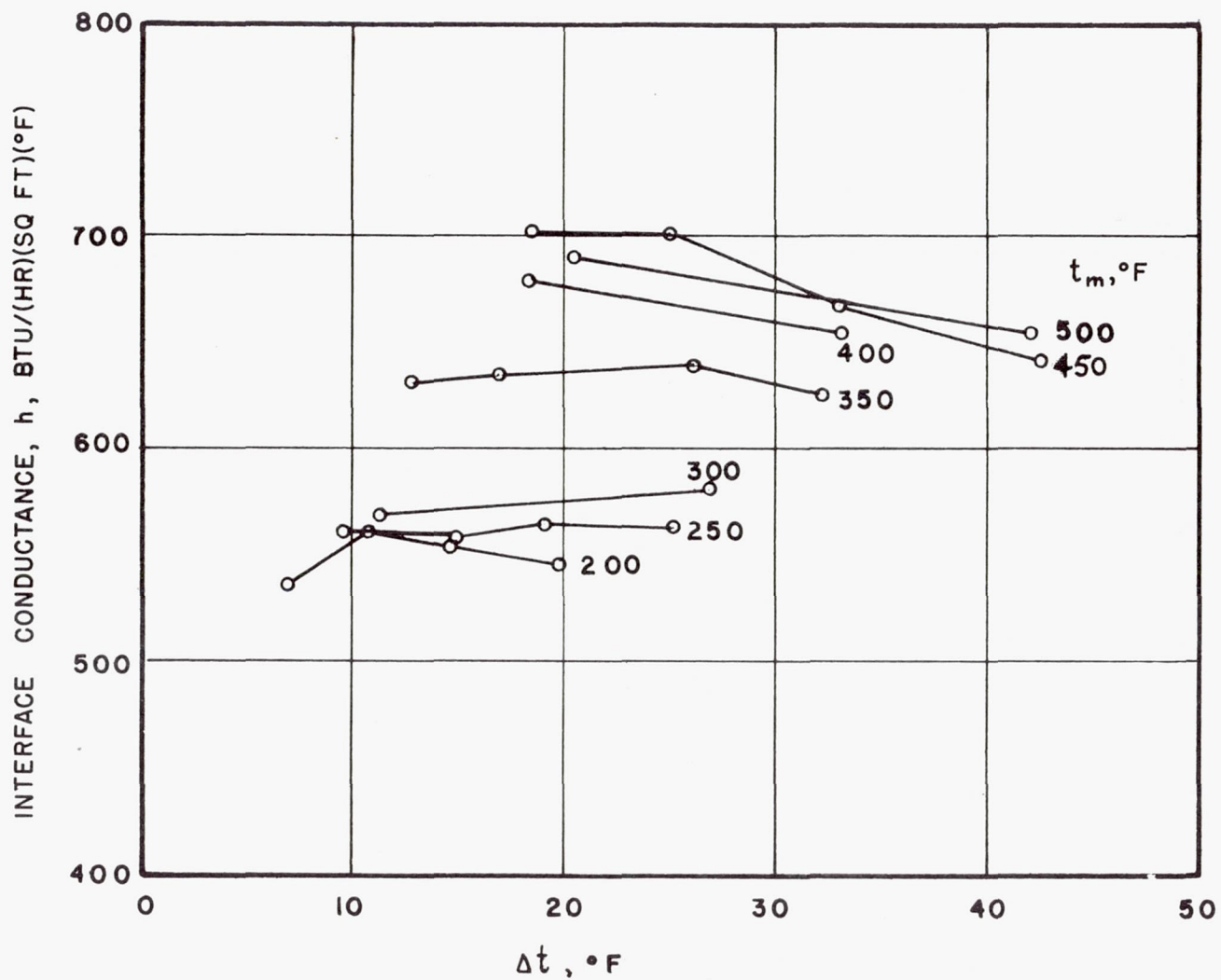
(c) Stainless-steel - stainless-steel joint (test 23).

Figure 7.- Concluded.
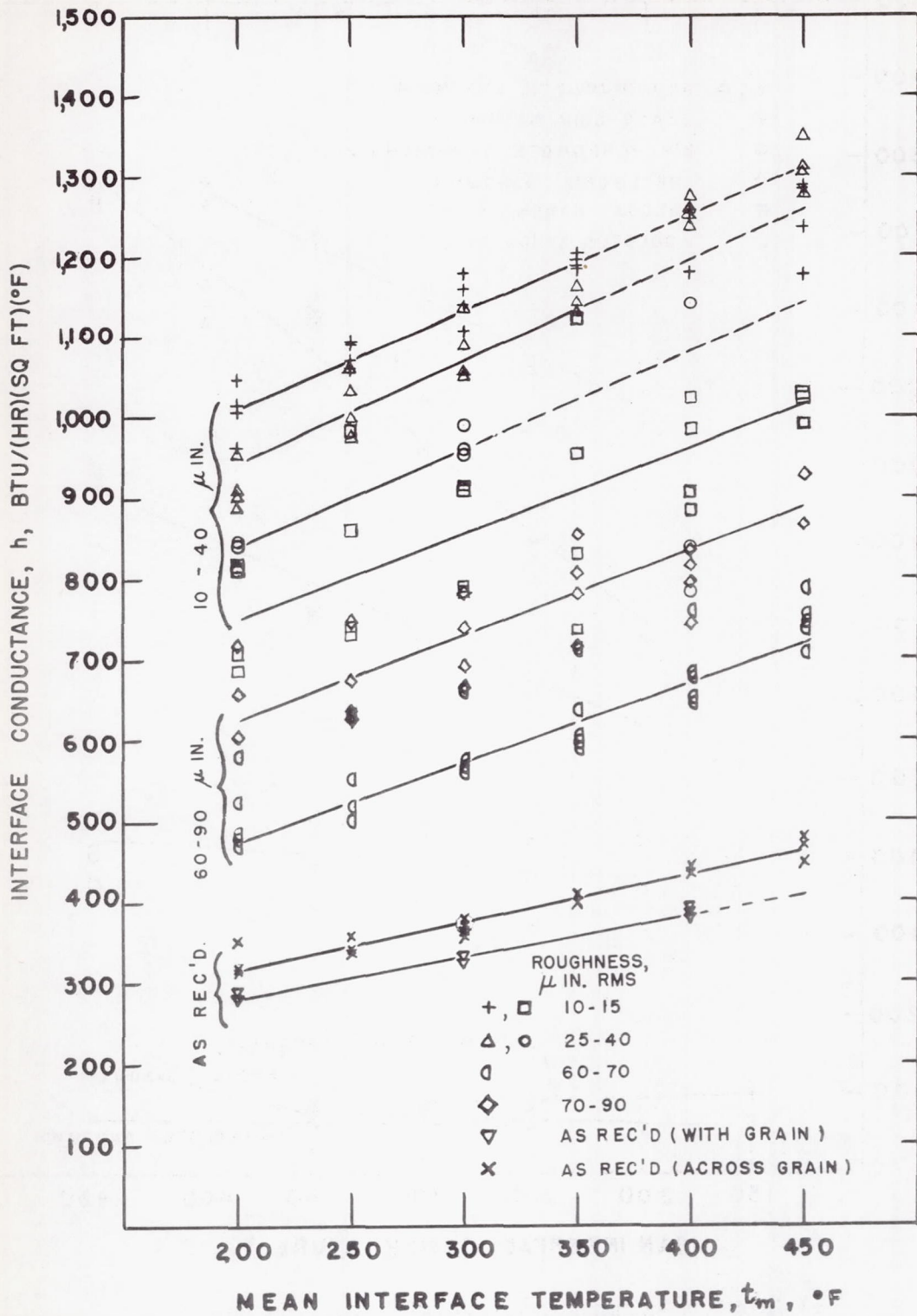
(a) Aluminum-aluminum joint with various interface roughnesses.

Figure 8.- Variation of interface conductance with mean interface temperature.
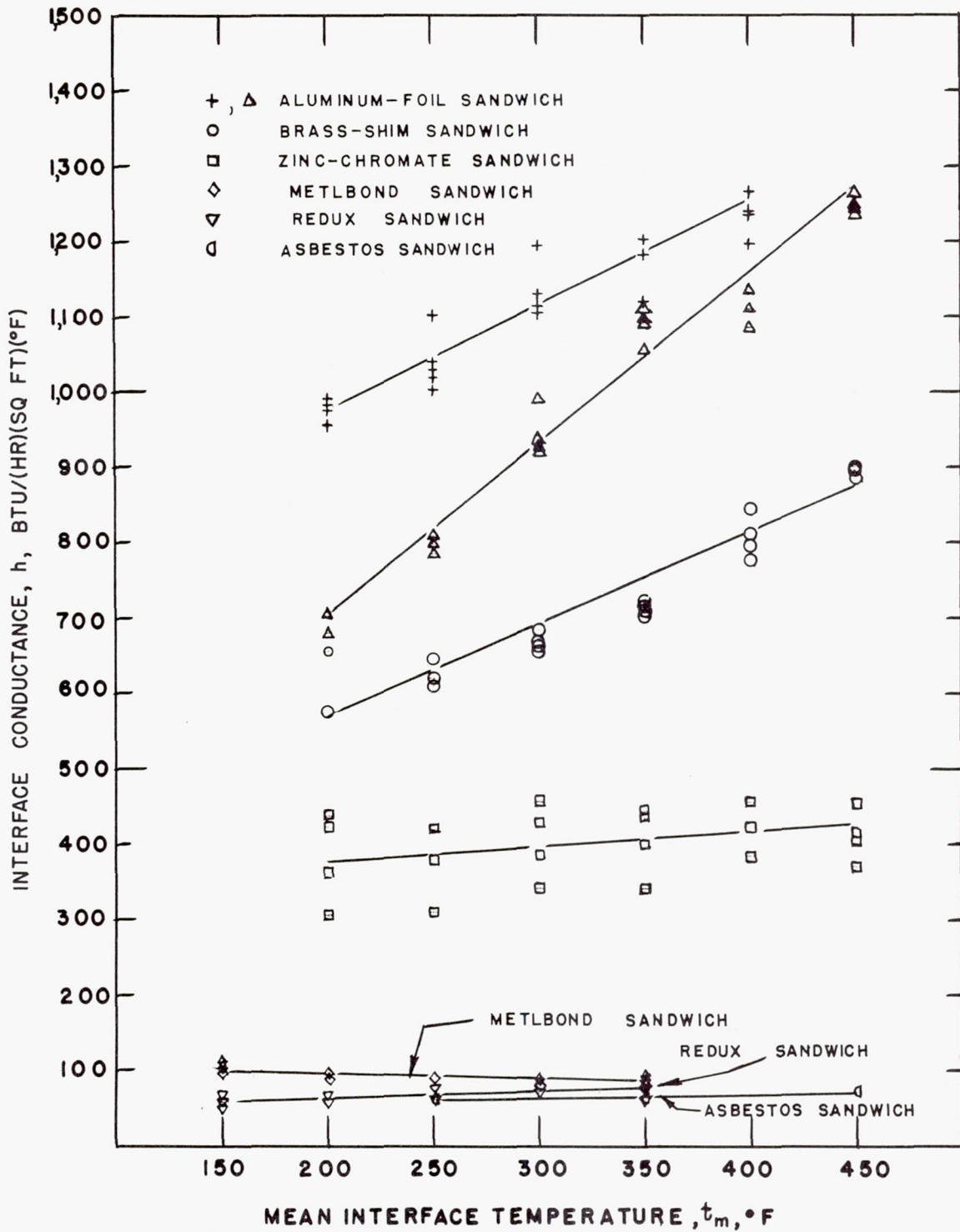
(b) Aluminum-aluminum joints with various sandwich
materials between interfaces.

Figure 8.- Continued.
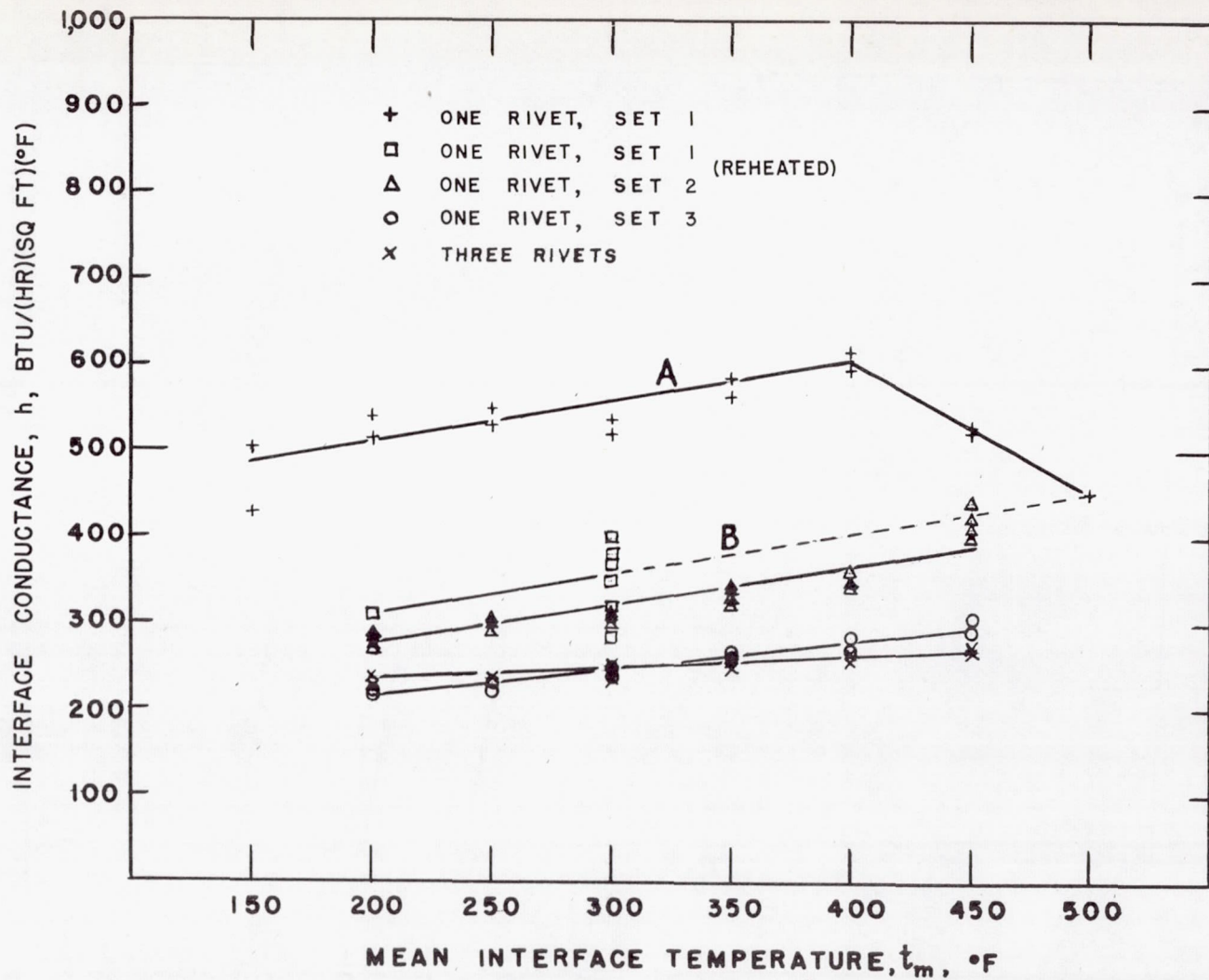
(c) Riveted aluminum-aluminum joints.

Figure 8.- Continued.
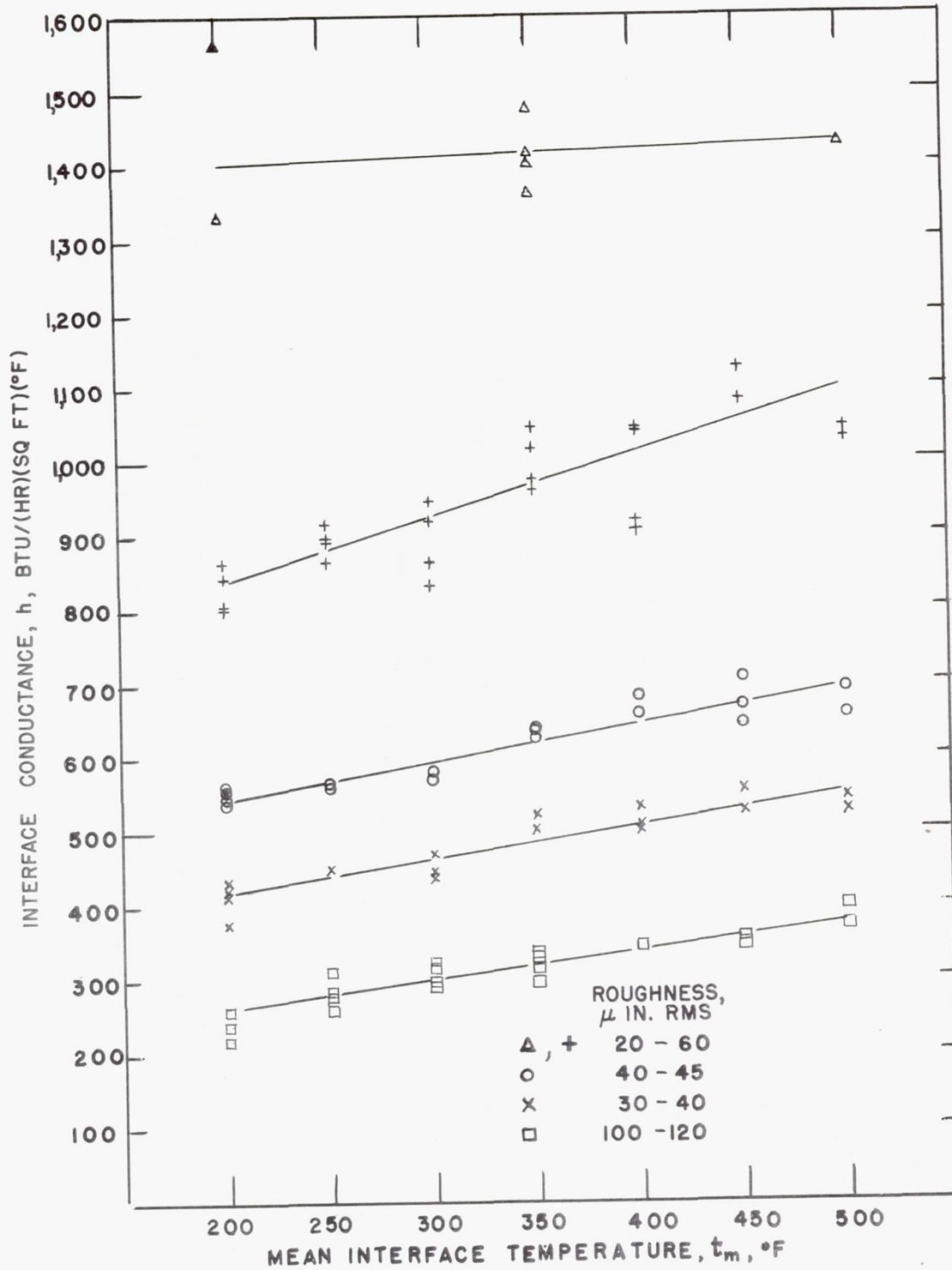
(d) Stainless-steel - stainless-steel joints
with various interface roughnesses.

Figure 8.- Continued.
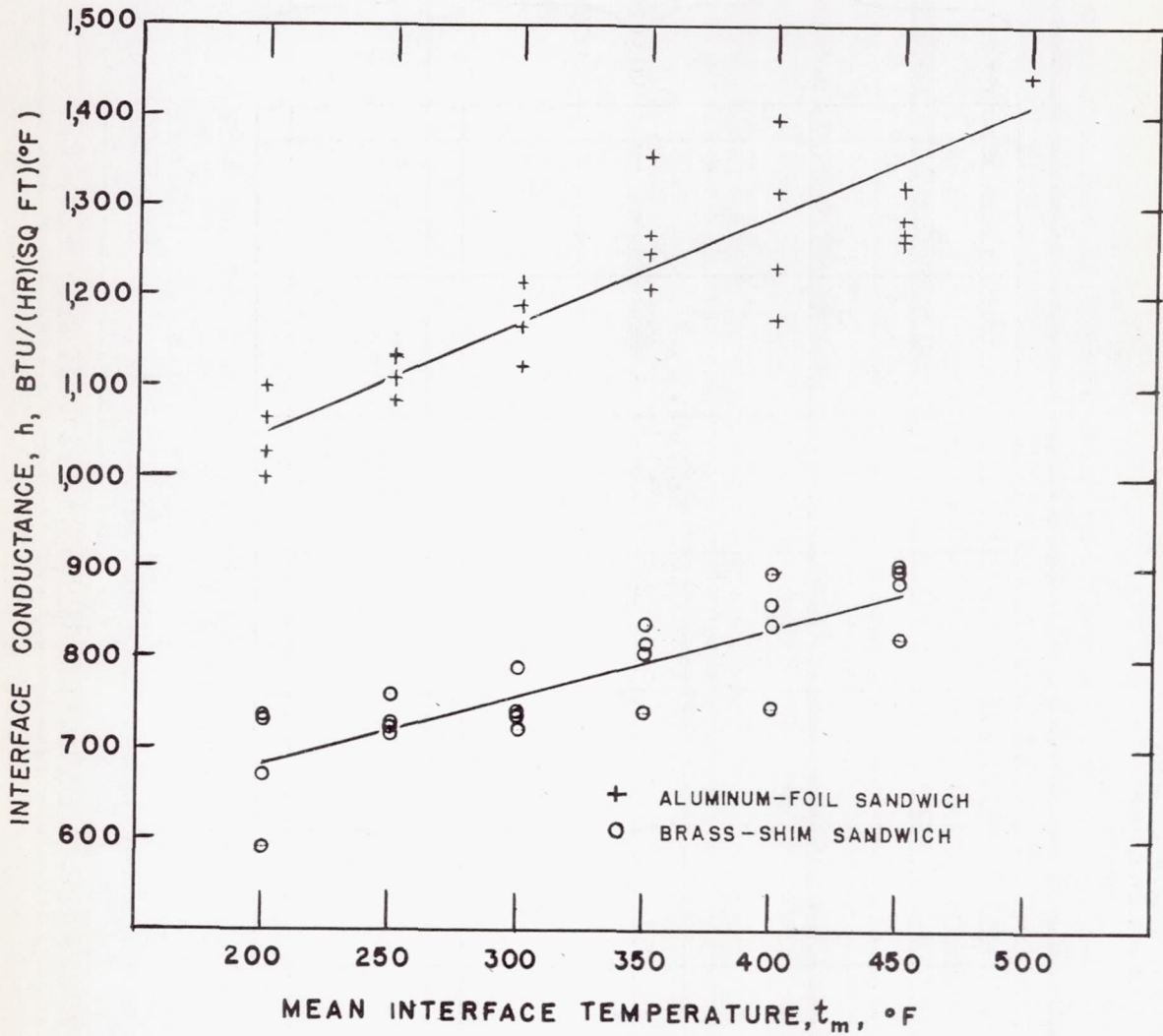
(e) Stainless-steel - stainless-steel joints with various sandwich materials between interfaces.

Figure 8.- Concluded.

TOP VIEW OF SPECIMENS
(SYMBOLS INDICATE LOCATION
OF THERMOCOUPLE ROWS
ALONG A VERTICAL LINE)
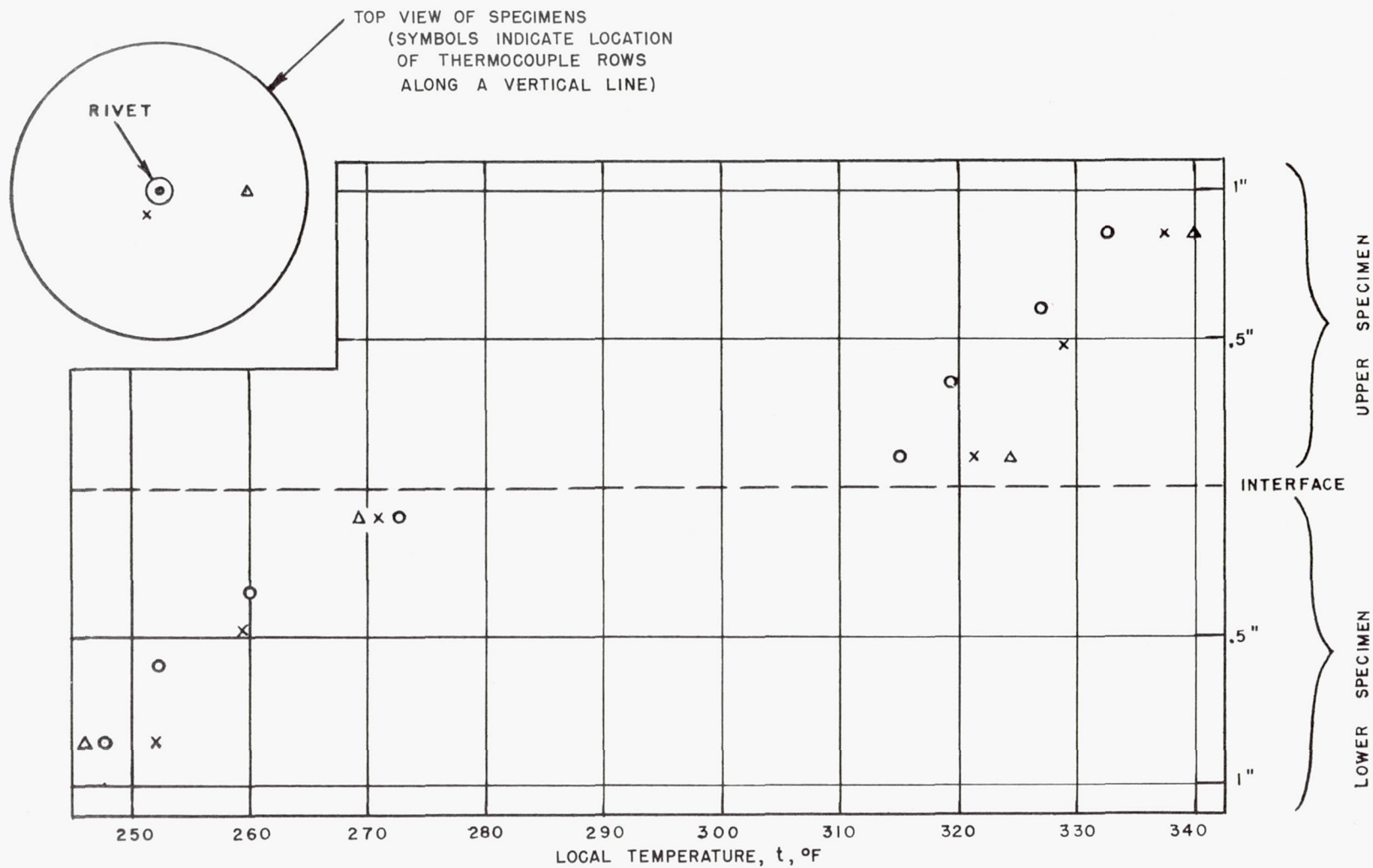
RIVET

(a) Single rivet (test 16).

Figure 9.- Temperature distribution in typical riveted specimens.

TOP VIEW OF SPECIMENS
(SYMBOLS INDICATE LOCATION
OF THERMOCOUPLE ROWS
ALONG A VERTICAL LINE)

RIVETS

UPPER SPECIMEN

1"

.5"

INTERFACE

LOWER SPECIMEN

.5 "

1"

250   260   270   280   290   300   310   320   330   340

LOCAL TEMPERATURE, t, °F
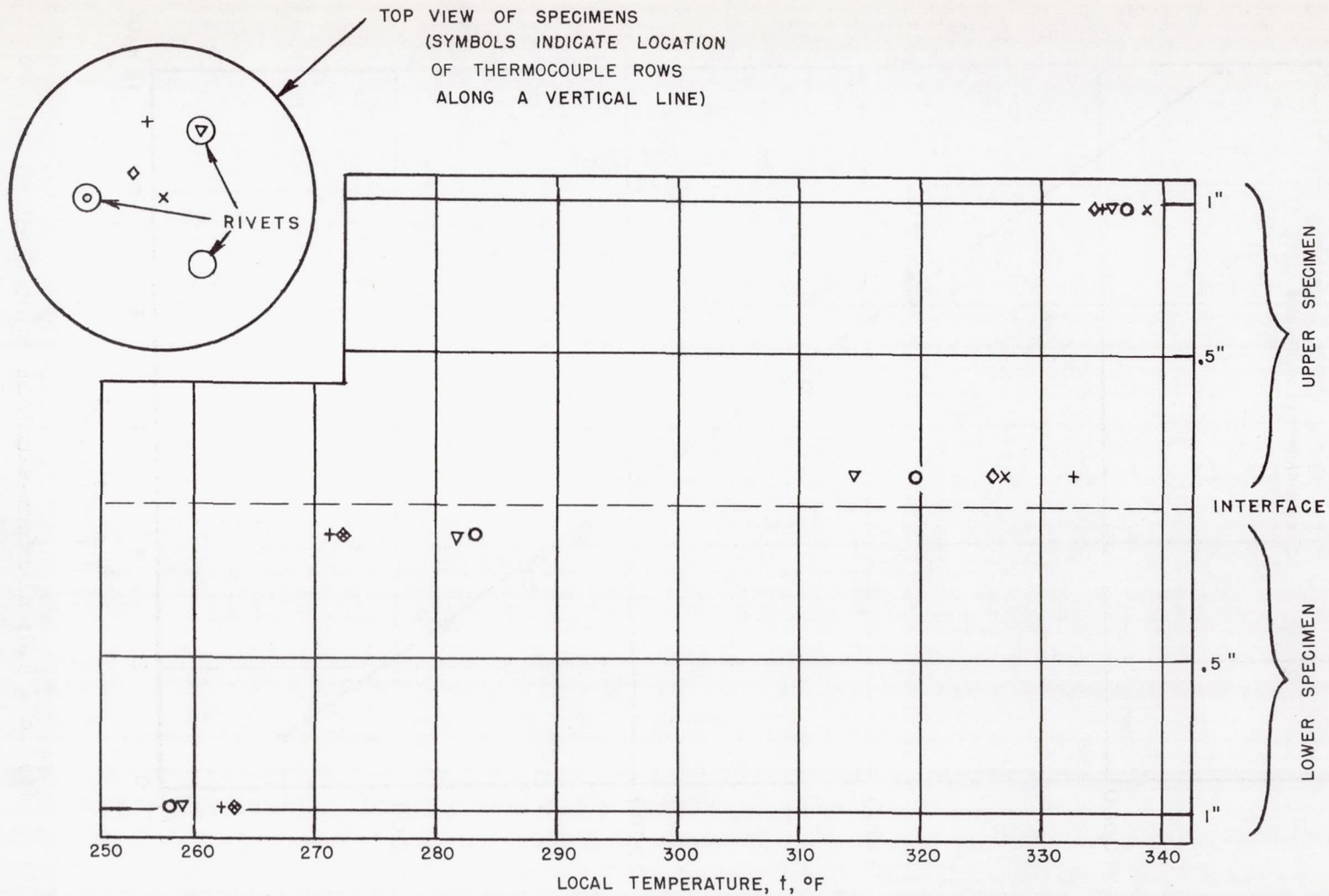
(b) Three rivets (test 20).

Figure 9.- Concluded.
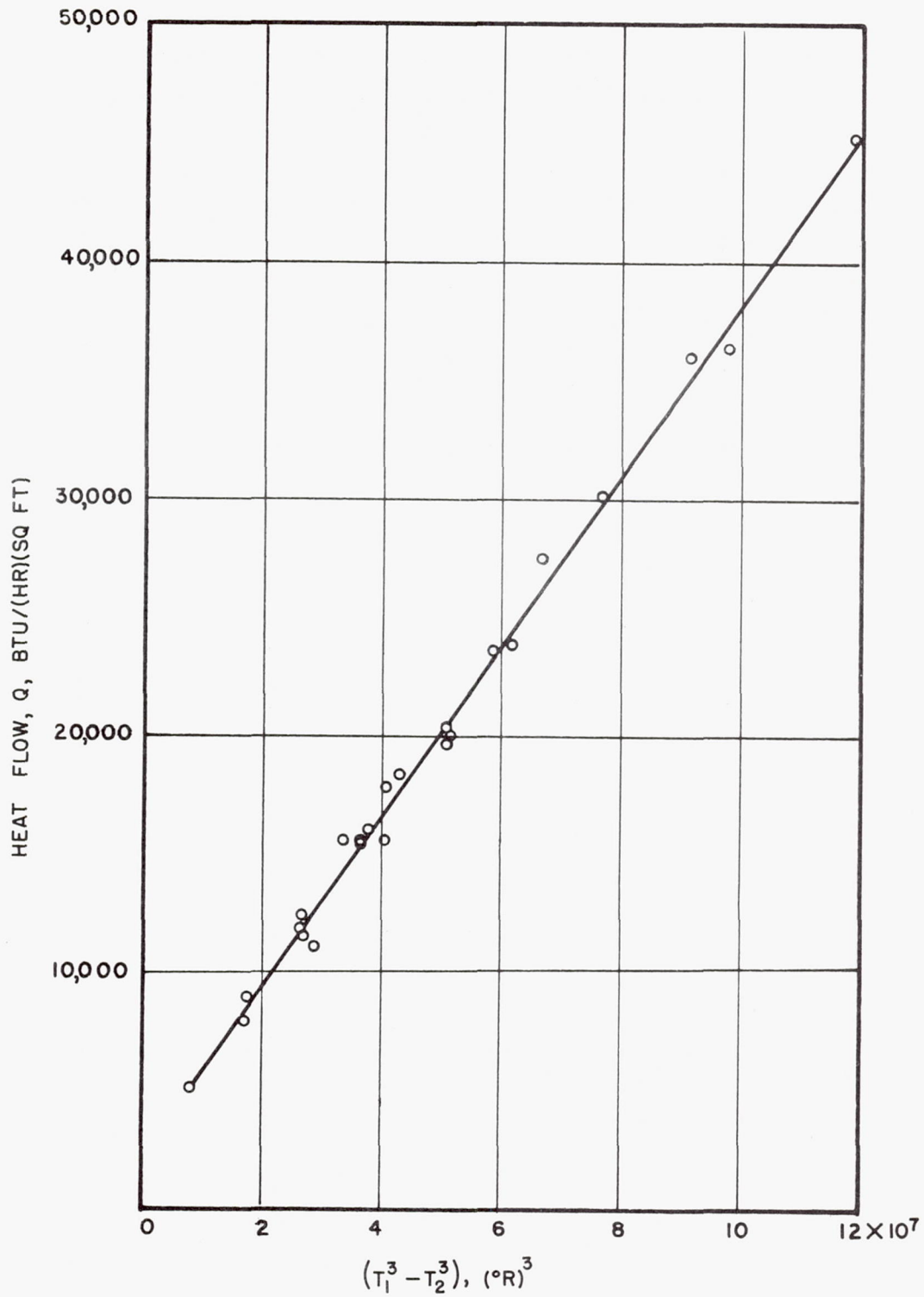
(a)   n = 3.0; aluminum-aluminum joint (test 5).

Figure 10.- Heat flow versus $\left(T_1{}^n - T_2{}^n\right)$.
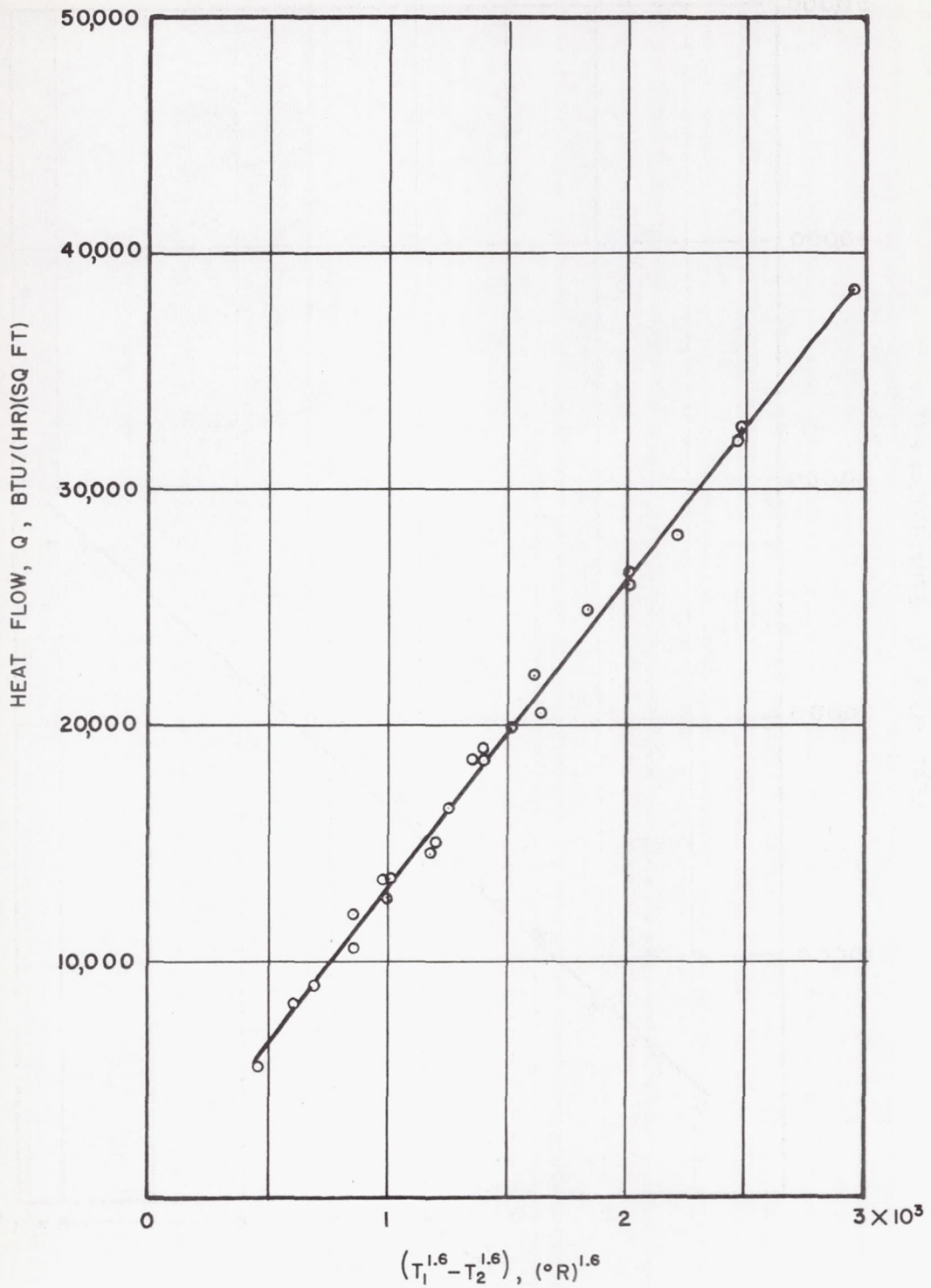
(b) n = 1.6; aluminum, aluminum-foil, and
      aluminum joint (test 9).

Figure 10.- Continued.
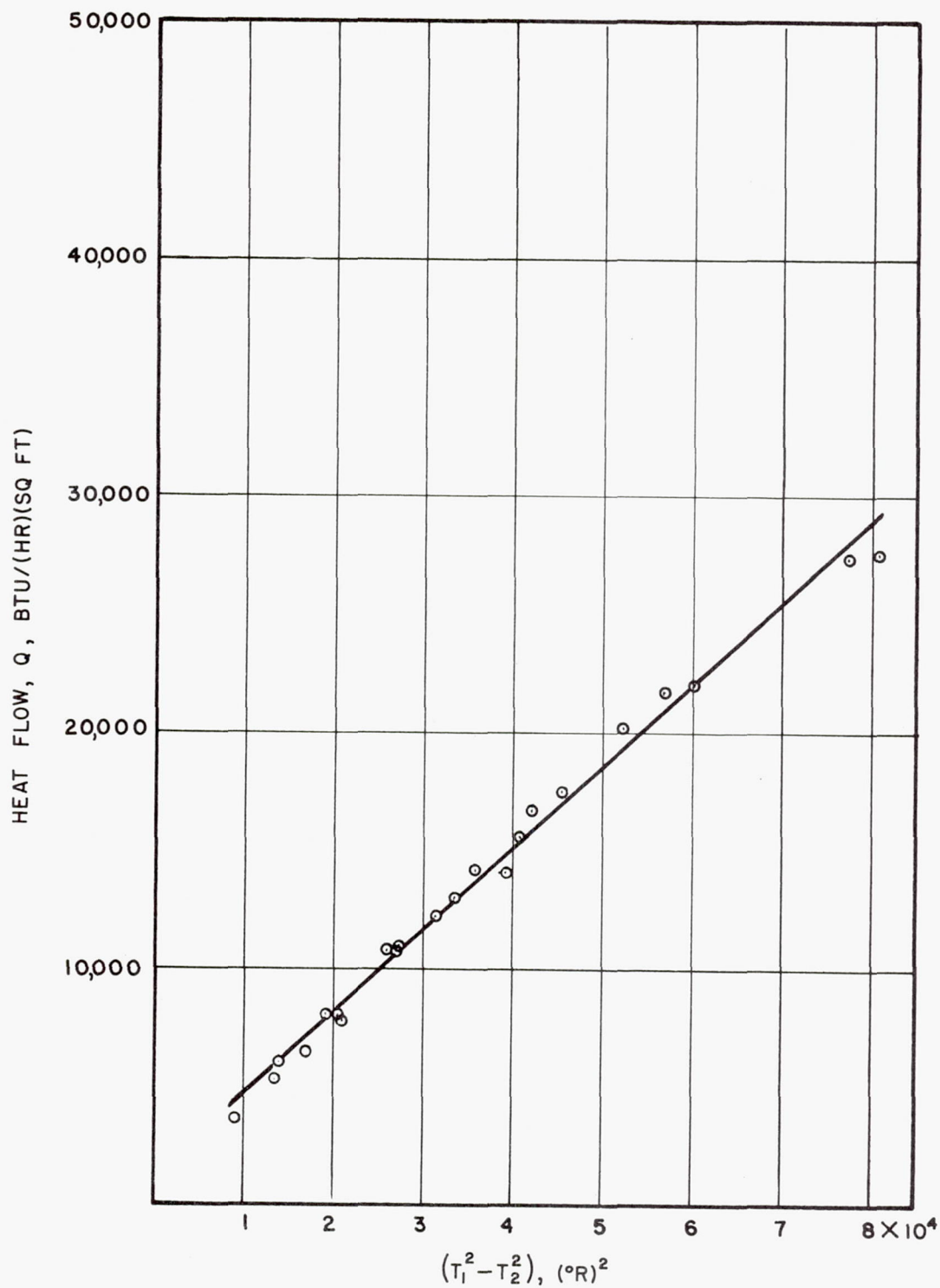
(c) n = 2.0; stainless-steel - stainless-
steel joint (test 23).

Figure 10.- Continued.
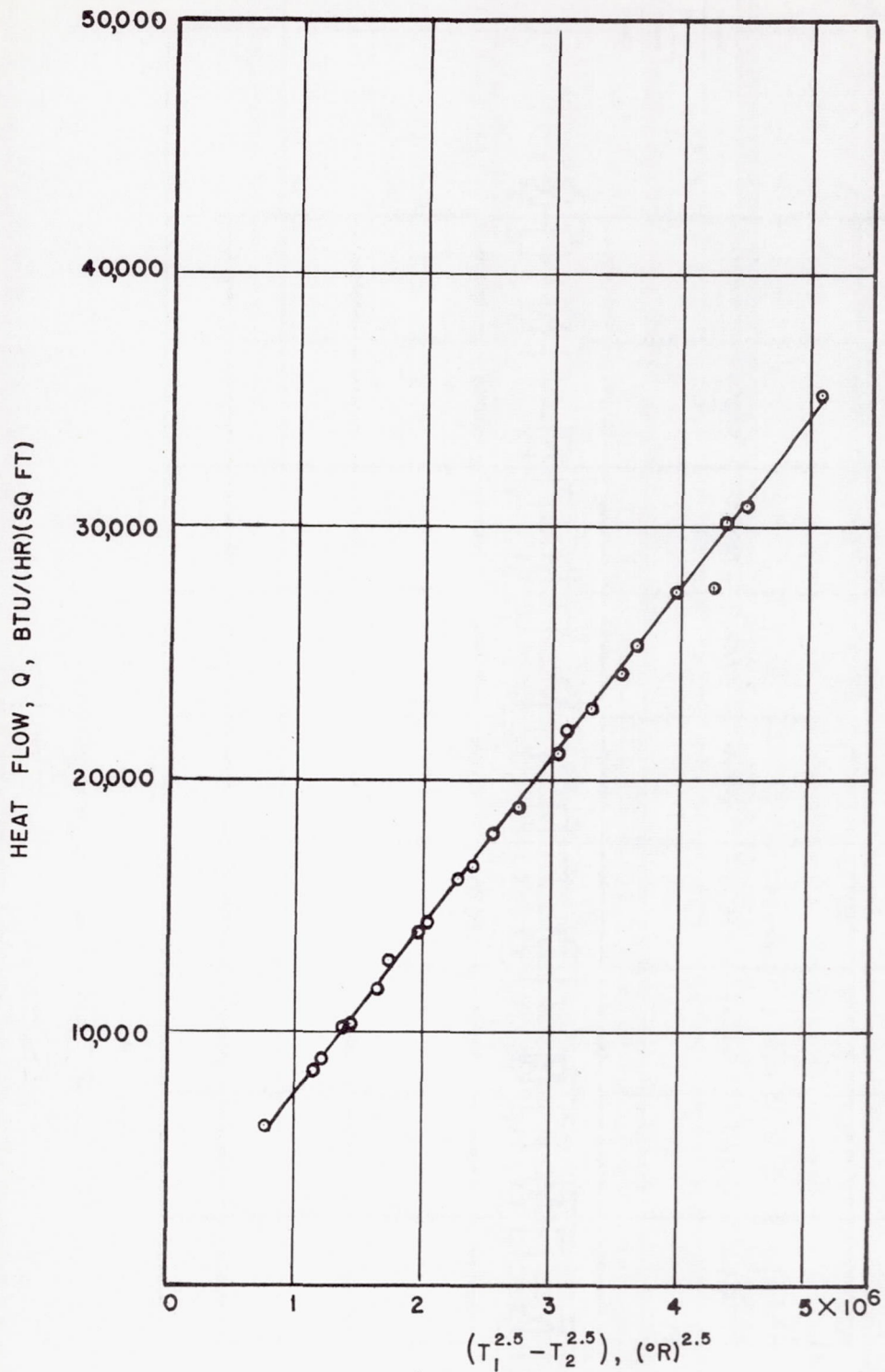
(d) n = 2.5; aluminum and aluminum, as received,
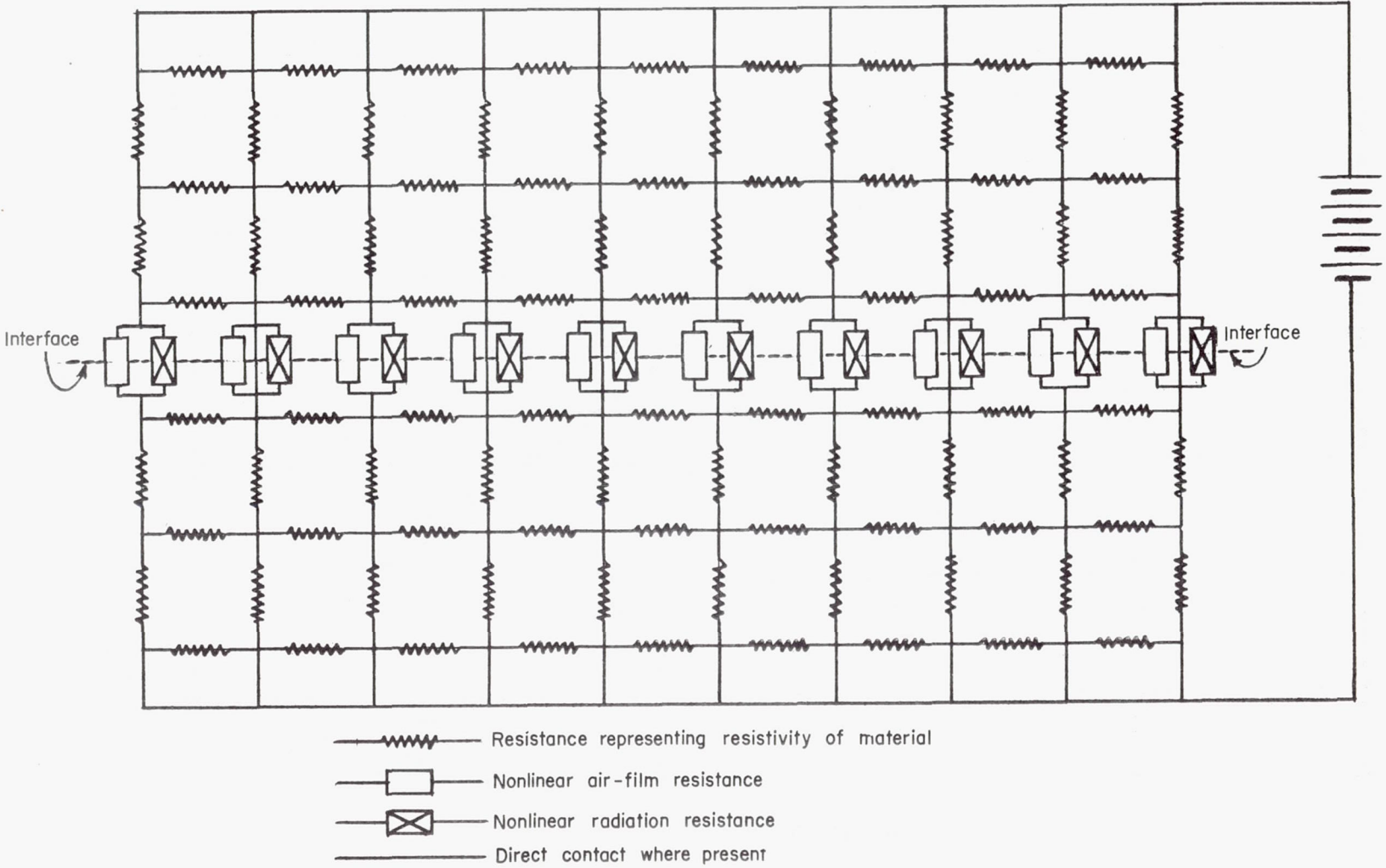joint (test 7).

Figure 10.- Concluded.

Resistance representing resistivity of material

Nonlinear air-film resistance

Nonlinear radiation resistance

Direct contact where present

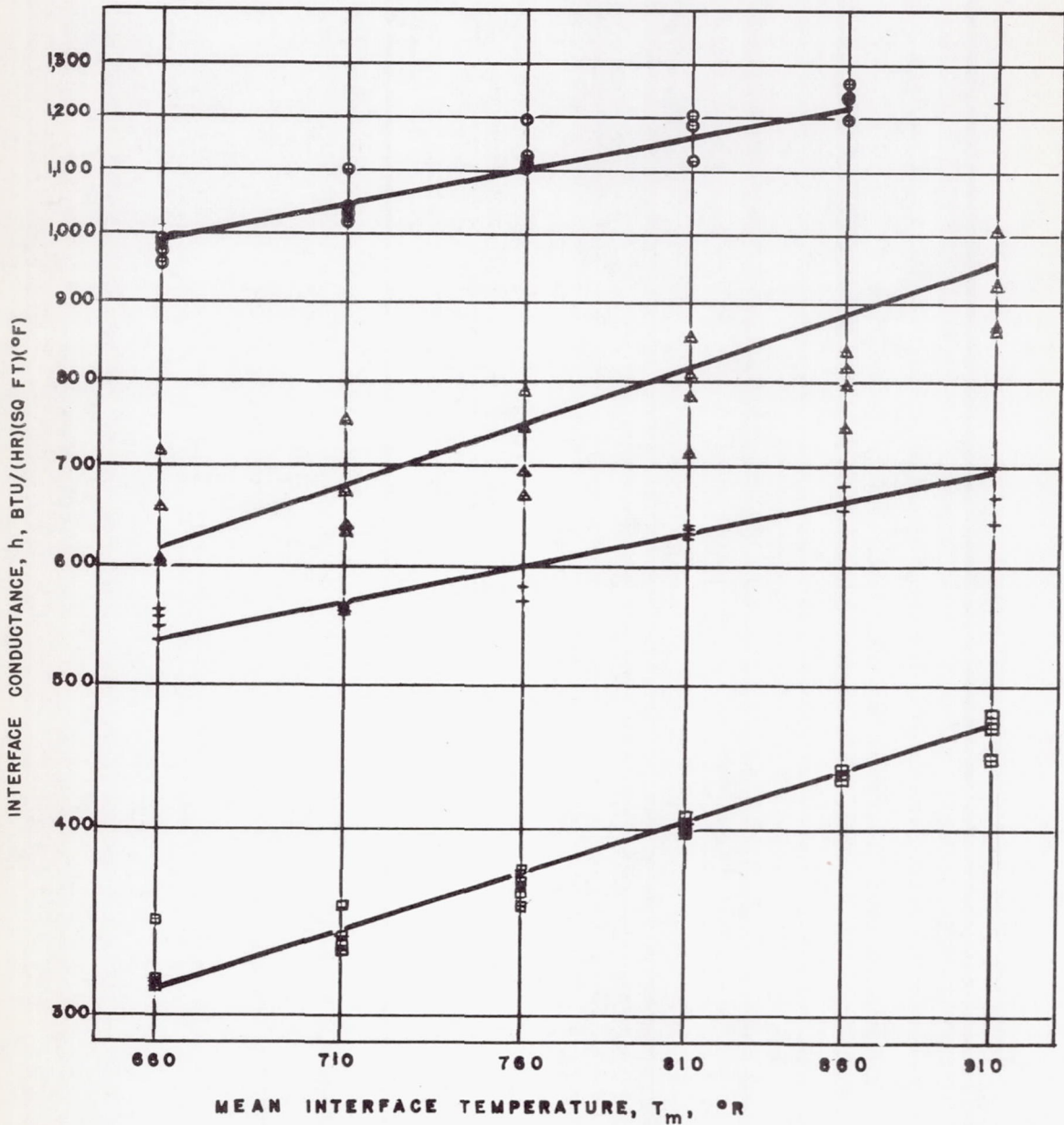Figure 11.- Electrical analog of heat transfer through interface.

Figure 12.- Logarithmic plot of variation in interface conductance with mean interface temperature.